

Assignment1
Subspace Signal Processing

Vangjush Komini
r0612470
vangjush.komini@uzleuven.be

September 7, 2016

Biomedical Data Processing Part II



1 Introduction

The underlying methodology of subspace signal processing is the decomposition of the signal into mutually orthogonal subspaces wherein one of them consist of the noisy subspace. This is ensured under the assumption that the signal itself contains two parts. One is the low-rank linear model for the "clean" signal and the additive uncorrelated (white) noise. Therefore the energy of the least correlated noise contaminating the whole signal is concentrated in a lower subspace compare to the highly correlated signal. Recovering the wanted signal after decomposition is performed by mapping the highly correlated subspaces onto the space where the structure is the closest to the clean signal. Additionally, the noise is supposed to be white before application of this decomposition, otherwise, whitening of the noise is required in case it is colored. This is possible with the noise covariance matrix to be known. Apart from filtering, subspace signal processing could also be employed for parameter estimation of an underlying estimation model. The outcome is significantly less biased compared to other existing methodologies, though they suffer from serious drawback. Very little prior knowledge is possible to incorporate into the framework. Last but not least, subspace signal processing enables simultaneous processing of multiple channels. This is an important feature since it is possible to benefit from cross-over information. Magnetic resonance spectroscopy MRS is one of the domains where subspace signals are heavily utilized. The general outline of the subspace signal processing is as follow:

- separate the ($\hat{H} \Rightarrow \text{signal} + \text{noise}$) subspace where the original signal $H = \hat{H} + W$
- suppress the ($W \Rightarrow \text{noise - only}$) subspaces from the noise only subspace.
- further suppression of the noise in the reconstructed space.

2 Artifact removal

Nuclear magnetic resonance (NMR) spectroscopy has the ability to select discrete region within the body for signal acquisition [?]. A radio frequency (RF) pulse presses the protons thus producing a free induction decay (FID) signal as in figure ???. This signal contains a lot of information regarding the metabolite activity in the region of interest (ROI). Since a human body mostly contains of water, thus, the water peak on the MRS spectrum has a much higher amplitude compare to the other metabolites ???. In order to observe the quantity of the rest of metabolites it is important to remove the water frequency component without distortion of the rest of the spectrum.

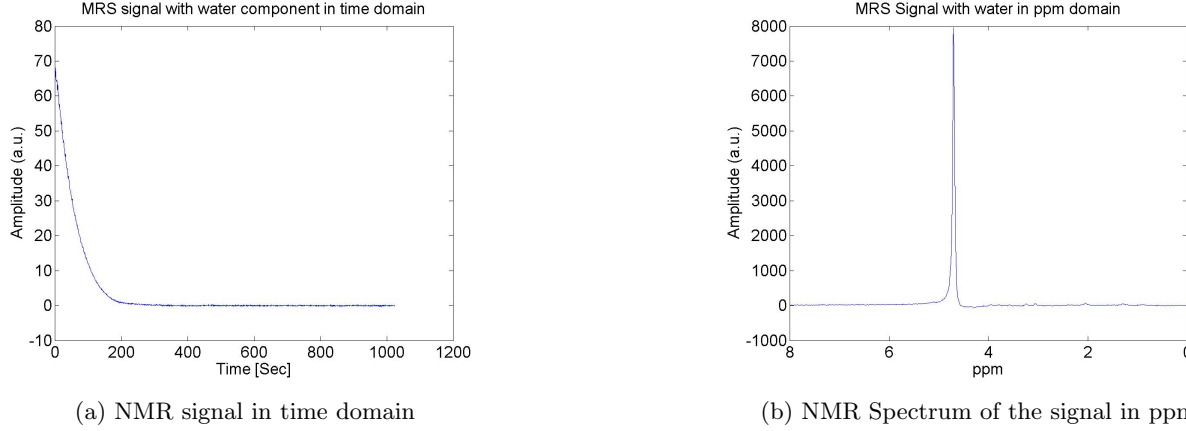


Figure 2.0.1: The raw signal acquired from the MRS

Water peaks on the NMR spectrum are considered to be an artifact and their suppression is achieved by omitting the decomposed component where their central frequencies is higher than 4.7ppm . This components has to be deduced from the original signal, whereby the rest of the desired metabolites will become more pronounced.

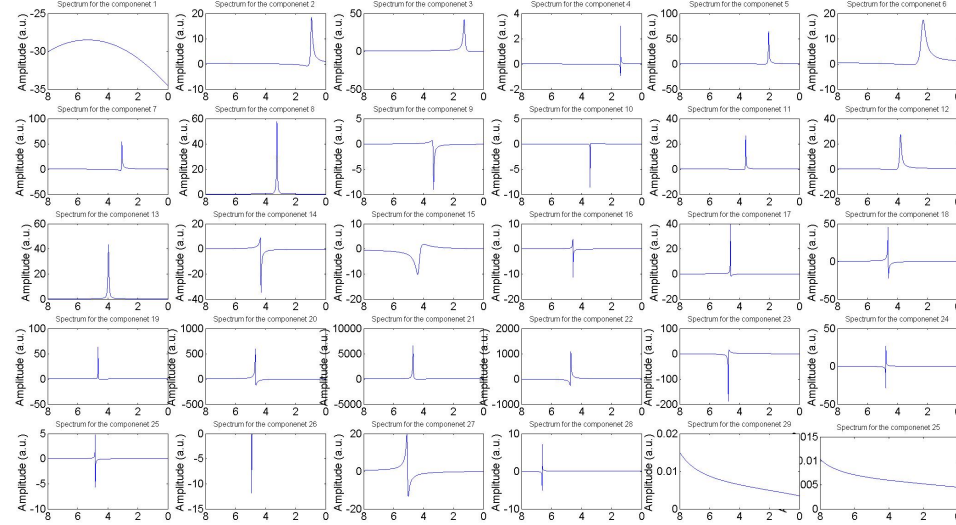


Figure 2.0.2: Individual components ordered on by the central frequency.

Hereby it is also very important to define the model order of the decomposition for high performance of artifact suppression. Two models order selection are being investigated. Minimum description length (MDL) and rank determination are two eligible methods for model order selection [?]. In figures ?? and ?? is the performance graph for MDL and rank determination method respectively. MDL indicates that that the higher the model order the better the performance of filtering and a similar result is provided from the rank determination.

A reasonable model order is necessary since underestimated model might omit the necessary pics needed to be suppressed. On the other hand, a very large order could generate unwanted spectrum including noise component [?]. In this case we have selected a model order of 29 since the it is a good moderation with the low processing complexity and the high performance.

The final signal for different model order could be found in ???. Whereas the filtered signal for the model order that suits the best for the implementation is in figure ?? with the water signal to be filtered out in the figure ???. The frame length luckily is much larger than the order of the signal model, therefore the correlation to be embedded could be fully explored[?].

Regarding the dimension ($L \times M$) of the Hankel matrix (H), a high number of rows (L) is required, given the orthogonality of signal (\hat{H}) and noise (W). This is on the beneficial to the noise removal from the approximation $\hat{H}W \approx 0$. This last

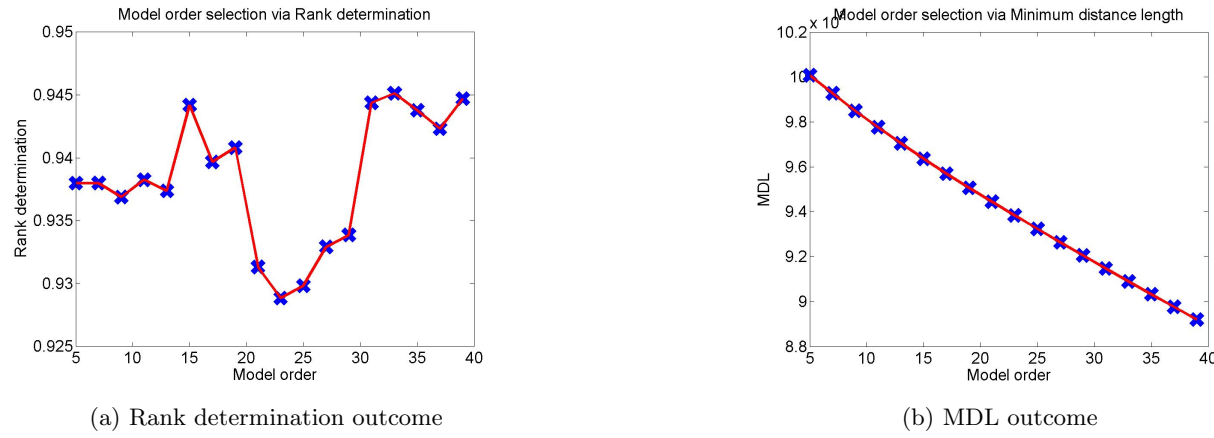


Figure 2.0.3: Model order selection

approximation in practice is not easy to be achieved, however, it approaches more and more to with the over-determination of the system. Therefore a $L >> M$ is necessary. However it has to be compromised with number of columns M , otherwise, a very large number of rows will reduce the number of columns being introduced. Therefore, this will worsen the approximation $H_n^T H_n \approx \sigma_v^2 I$ [?]. The best performance and accuracy of the system is obtained when the Hankel matrix is a rectangular case. This will speed up the processing time of the KarhunenLove Transform (KLT) and it compromises the number of rows and the number of columns.

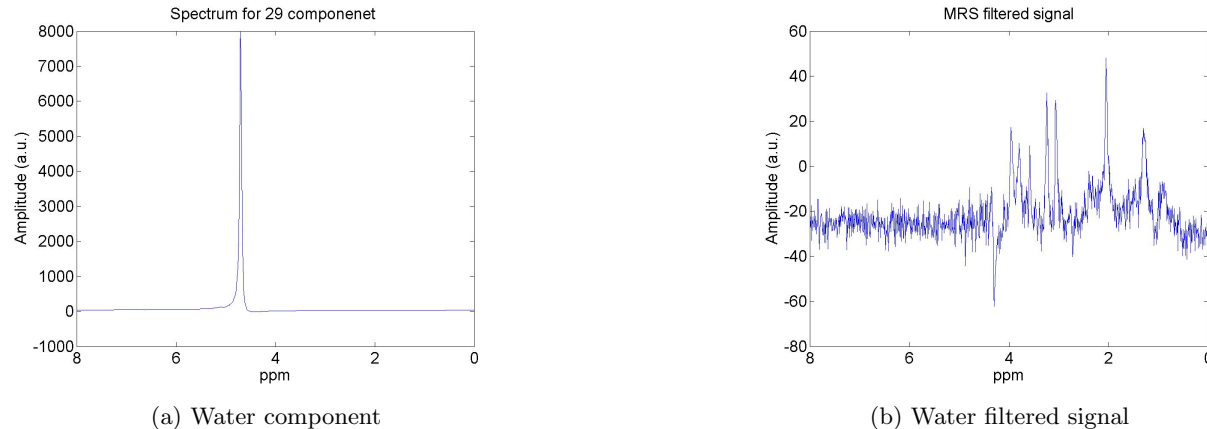


Figure 2.0.4: Final results

The water filtering is done by removing the water component in figure ?? from the original signal spectrum in figure ??.

2.1 Comparison with classical filters

- The superior benefit of subspace filtering consists in its ability to recover the clean signal with the minimum distortion as well as the minim residue noise possible. In spectral based and Wiener filtering approach, the noise removal is a process which also introduces distortion to the wanted signal. This obstacle is overcome in subspace methods by nulling the noisy subspace which has no mutual information with other desired subspaces. Additionally, the noise accumulated in the subspace to be nulled is on higher amount compare to amount of noise being suppressed via the spectral methods [?].
- Spectral based method is restricted by a fixed Fast Fourier Transform (FFT) computing whereas Singular Value Decomposition (SVD) based topologies vary in computational time with the KLT data. In addition, KLT transform $O(nm^2)$ is far more heavy in terms of computation time compare to FFT $O(nlog(n))$ [?].
- Moreover, in this content subspace methods assume explicitly the order of the signal, or in other word the rank-deficient speech observation matrix. Whereas Wiener filtering does an implicit rank reduction based on a estimation of rank reduced correlation matrix [?].
- Apart from the FFT spectral based, Discrete cosine transform (DCT) is another candidate for signal enhancement. Yet it is far superior compare to the theoretical subspace filtering[?].
- Differently from the classical filters, subspace methods efficiency depend significantly on the ability of the user to identify the accuracy of the characteristics of the underlying signal. The better the properties are defined the better the removal of the noises is performed[?]. The other classical filters require no need of any additional visualization skills, therefore, are mostly applied in fully automated framework.

- In order to consistently apply the subspace filtering, the signal has to be modelled into a clear analytical formulation. In some modalities this is not a very easy task consequently its application is restricted into very well known physical models.
- Another fundamental issue with subspaces signal is that noise incorporated in the signal which needs to be reduced is considered white. In case of narrow band noises a pre-whitening step has to be applied before the filtering itself takes place, given the noise covariance matrix is known [?].

3 Parameter estimation

In order to apply subspace methods for parameter estimation, an underlying model has to be utilized with well defined parameters. Exponentially damped sinusoidal (*EDS*) is a very convenient model and widely utilized in different signal processing applications figure ???. Hereby the signal being detected in the sensing device is modeled as a superposition of damping signals at distinct frequencies contaminated with white Gaussian noise (*wgn*) equation ???. These components accommodate the information regarding the tissue properties, therefore accurate estimation of the amplitude a_k , frequency f_k , phase ϕ_k and damping d_k is very critical. The analysis is performed in the frequency domain.

$$y(t) = \sum_{k=1}^K a_k \exp(j\phi_k) \exp(-d_k t + 2\pi f_k t) \delta t + wgn \quad (3.0.1)$$

Utilizing the estimated parameter, a modeled signal (*EDS*) is then employed for peaks of interest computation . Via subspace methods based on (total) least square approximation a best fit between the modeled and the original signal is computed. This will enable a good estimation of peaks closely spaced,as well as their amplitudes.

Herein the main algorithm being introduced is outlined in ?? which fits the model either via least square (LS) or via total least square (TLS). Additionally prior knowledge of poles are also being incorporated in the algorithm for further increase of the accuracy of the estimation. In order to validate the robustness of the methods, *wgn* is superimposed to the water filtered signal and the estimated parameters are then compared to the *wgn* free signal.

Contrary to LS solution which introduces higher bias and inconsistency, TLS methods introduce an asymptotically bias compare to the ground truth solution [?]. The known poles will enable the orthogonal projection of the data via QR decomposition whereby it will remove the known part ??.

In figure ?? are the spectra of the reconstruction signal from the noise free signal respectively to the three methods. Whereas on the figure ?? there are the spectra of the reconstructed signal from the noisy signal for respective method.

The performance of each method is outlined in the table ???. The first row corresponds to the absolute mean value of the difference between the original and the fitted signal $\Delta = Signal - Fitted$. Herein there is a clear evidence that the mean value will increase for the same method from the pure to the noisy signal. This is the effect of the noise contamination which will worsen the performance of the method. The noise impact is also noted in the variance of Δ where the variability increases with a small factor in the noisy signal case.

In case of method comparison, root-mean-square-error (RMSE) has been chosen as a good indicator. In the figure ?? HSVD curve on average tends to stay above the other models. Thereby indicating a higher bias incorporated into the estimation. On the other hand, *HTLSPKF D* outperforms HTLS based on the same graph in figure ???. Herein the RMSE tends to oscillate significantly for high level of noise and stabilizes the signal level significantly higher. However, on average the error introduced by *HTLSPKF D* sits on lower values as compared to the HTLS case and HSVD.

The residue signal for each estimation is plotted in the figure ??, whereas the individual component superimposed together for the modeled signal are in the section ???. The estimated parameter including amplitude, frequency, phase and damping via respective method are listed in the section ??.

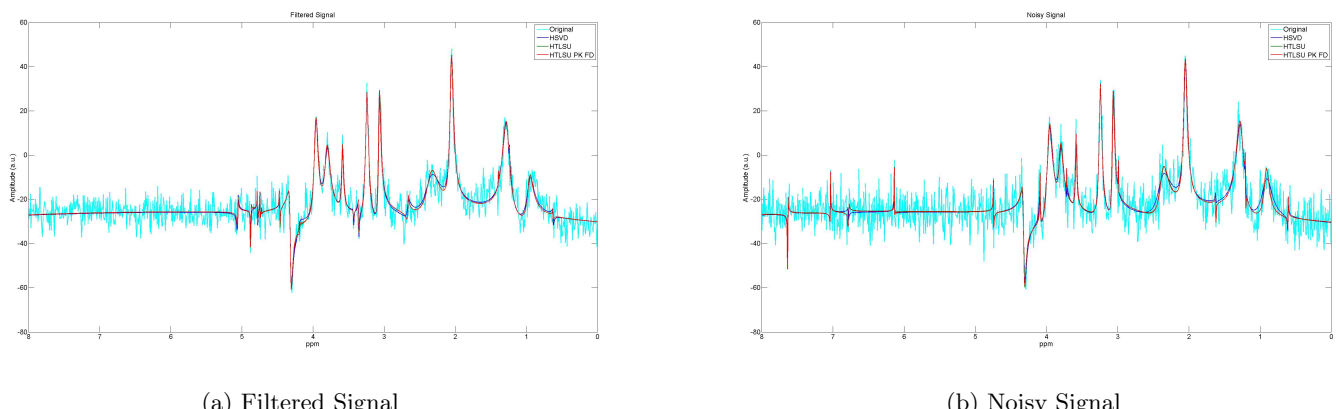


Figure 3.0.1: Reconstruction Outcome

Table 1: Fitted performance

	<i>HSVD</i>	<i>HTLS</i>	<i>HTLSPKF D</i>	<i>HSVD</i>	<i>HTLS</i>	<i>HTLSPKF D</i>
	<i>Puresignal</i>	<i>Puresignal</i>	<i>Puresignal</i>	<i>Noisysignal</i>	<i>Noisysignal</i>	<i>Noisysignal</i>
<i>Mean</i>	5.928808e - 04	6.241688e - 04	5.415201e - 04	1.451811e - 03	1.228149e - 03	1.326272e - 03
<i>Var</i>	1.976946e - 02	2.017998e - 02	2.015972e - 02	2.200519e - 02	2.384214e - 02	2.430506e - 02

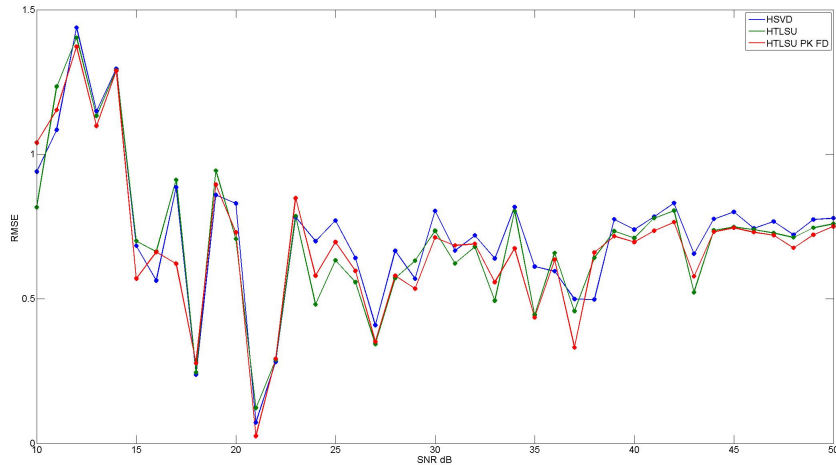


Figure 3.0.2: Reconstruction Outcome

3.1 Subspace methods for parameter estimation

- In subspace method it is very hard to incorporate prior knowledge of the parameters to be estimated. However, in [?] and [?] the algorithm is proposed as an extension of HTLS capable of accommodating prior knowledge in the computation. It will increase the accuracy together with the resolution. Whereby it will facilitate the estimation of closed spaced peaks in the NMR spectrum with values very close to the Cramer-Rao (CR) lower bounds. The reason why the CR bounds became smaller is due to the non-zero mutual uncertainty of the parameters to be estimated. A further investigation is introduced in ??.
- Subspace methods on the other hand are very robust framework. On other word it is a well-posed problem solution. It means that the solution exist and it is unique, nevertheless the solution is very sensitive to the initial conditions [?].
- Additionally the subspace methods are not iterative methods as compared to other optimisation based existing methods. Herein there is no cost function to be iteratively minimized, consequently the reproduction of data is ensured[?]. The time complexity is much lower compare to optimisation based methods.
- Subspace based methods, however, don't suffer from local minimum. This is ensured from the lease square method wherein the best solution is outcomed.
- The user capability to initialize the parameters of the subspace methods is very important. In case of MRS signal the number of peaks are visually estimated. This restricts the method from being fully automatized.
- Furthermore, subspace methods are capable for parameter estimation of multiple different signals at the same time via the extension of the existing HTLS based algorithms[?]. Consequently big data could be processed simultaneously instead of an iteration over single signal in the optimization case.

4 Noise removal

Apart from artifact suppression, subspace methods can be further employed for the additional enhancement of the signal. The signal represented into a (\mathbf{H}) Hankel data matrix could be seen as superposition of the \hat{H} exact signal and the (W) pure noise. Taking into account that **wgn** is fully orthogonal to the signal to be estimated. Using an analogy of multivariate version of Pythagorean lemma for triangle, it is possible to recover the clean signal. Whereby the exact noise could be recovered via SVD as follow:

$$\hat{H} = \hat{U}\hat{\Sigma}\hat{V}^h = [\hat{U}_1\hat{U}_2] \begin{pmatrix} \hat{\Sigma}_1 & 0 \\ 0 & 0 \end{pmatrix} [\hat{V}_1\hat{V}_2] \quad (4.0.1)$$

$$H = U\Sigma V^h = [U_1U_2] \begin{pmatrix} \Sigma_1 & 0 \\ 0 & \Sigma_2 \end{pmatrix} [V_1V_2] \quad (4.0.2)$$

This estimation is possible under the fulfillment of the following conditions:

- the clean signal is orthogonal to the noise $\hat{H}^T W = 0$
- orthogonality of matrices \hat{V}_1 and \hat{V}_1 must be preserved in the inner product $\hat{V}_1 W^T W \hat{V}_2 = 0$ ¹
- the smallest singular values σ_k ins Σ_1 have to be larger than the largest noise singular value σ_{K+1} in the Σ_2

Noise separation performance depends critically on the the three criteria above, which in practice are never achieved, apart for the last condition. In order to satisfy the first criteria as the most important one it could be seen as an optimisation method. Minimizing the cost function in equation ?? is completed by computing the transformation matrix T such as:

$$\min \|HT - \hat{H}\|^2 \rightarrow T = (H^T H)^{-1} H^T \hat{H} \quad (4.0.3)$$

This estimation is known to be the minimum variance (MV) [?] which gives the orthogonal projection \hat{H} into the column space of H . Combining equations ?? and ?? the final estimation is equated as below:

$$HT = UU^T \hat{H} = U_1 U_1^T \hat{U}_1 \hat{\Sigma}_1 \hat{V}_1^T = U_1 (\Sigma_1^2 - \sigma_w^2 I_K) \Sigma_1^{-1} V_1^H = U_1 (\Sigma_1^2 - L \sigma_v^2 I_K) \Sigma_1^{-1} V_1^H \quad (4.0.4)$$

Herein can be seen that the system is introducing a bias in the estimation as far as $U_1 \neq \hat{U}_1$ and $\sigma_v^2 = \frac{1}{L(M-K)} \sum_{i=K+1}^M \sigma_i^2$ is the average value of the noisy singular values. An outline of this algorithm could also be found in ?. This method is a further improvement of Cadzow algorithm [?] where the estimation is performed as $HT = U_1 (\Sigma_1) V_1^H$.

Apart from single channel method, multichannel Cadzow MCC is also executed in here for comparative studies, where the NMR signals from different voxel locations are utilized [?]. The voxels are the neighbours of the voxel of interest (VOI) which are located around into a horizontal cross-section. The method is also outlined in the section ?? adapted from [?] and [?]. This multichannel algorithm could further be enhanced (Multi-Channel Cadzow Enhanced (MCCE)) by taking into consideration different model order as well as different neighbouring size (3x3,5x5,7x7). In addition, different neighbour method is also investigated counting here square, diagonal and antidiagonal positioning. These four algorithm are executed on the data samples from NMR signal acquired in a human brain for 1024 voxels (32x32).

In order to quantify the performance of each algorithm the signal-to-noise level is computed via equation:

$$SNR = 20 * \log \left\{ \frac{var(Signal_{Filtered})}{var(Noise_{Residue})} \right\} \quad (4.0.5)$$

$Noise_{Residue}$ is the last 200 (arbitrary) sample of the filtered signal since in the FID case the main signal is at the beginning of the induction. Whereas the oscillation in the signal happening at the very end are considered noise since they do not come from any activity in the brain.

After removing the water component from all the signals at different voxels as in section ?? the enhancement of the signal is performed via Cadzow, MV, MCC and MCCE and the results are outlined in figure ?. Furthermore, the parameter estimation for respective signal is performed using HTLS method as in the section ?? and the table of values are listed in section ?. Via the parameter estimated for each algorithm the reconstruction signal is obtained. The result of the reconstructed signal are drafted in figure ??.

Table 2: SNR evaluation for different methods

	Signal	Cadzow	MV	MCC	MCCE
SNR	31.3230	61.2315	64.9762	68.9809	98.9809

As it is expected the SNR value increases after applying Cadzow as the first enhancement algorithm. The SNR is higher case of MV as compareD to Cadzow since the filtering of noise is higher due to the higher reduction of the principal singular values in equation ?. Furthermore, the multichannel algorithm yields better performance as compare to the both Cadzow and MV since it takes into account 3x3 neighbours. Overall, the MCCE outperforms the previous methods since it has been optimized over the three parameter models, model order, neighbouring distance and manner. The MCCE is indicated to have the best performance for model order of 26 over a neighborhood of 7x7 for in an square orthogonal manner.

¹ $W^T W = \lambda I$

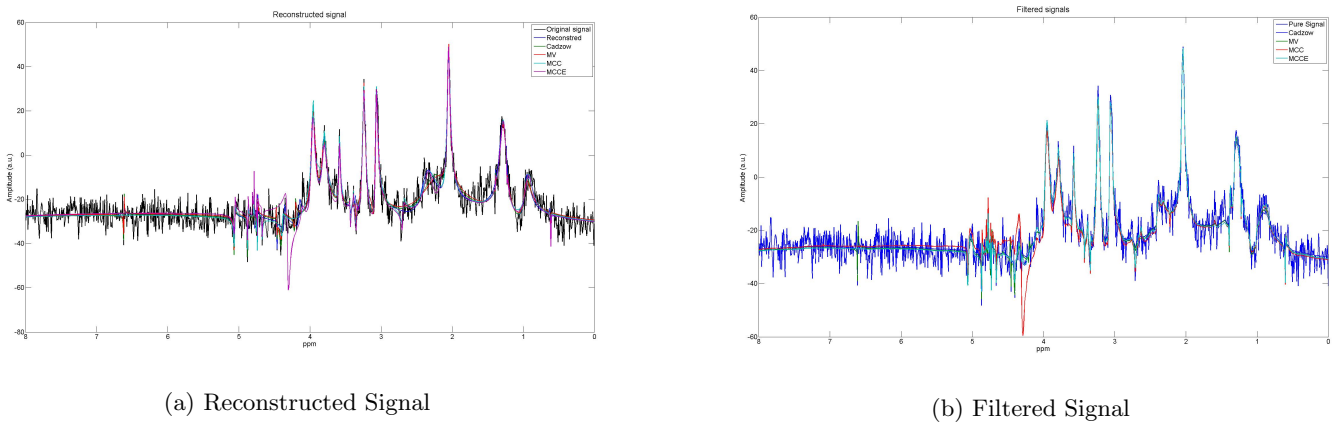


Figure 4.0.1: Final results

4.1 Cadzow vs Minimum Variance

These methods are intrinsically quite similar to each other with the main difference that instead of computing the LS solution for the signal it does compute the minimum variance MV equation ?? . Whereby the first criteria is better approximated with MV. In this way the separation of noise outperforms Cadzow algorithm since the orthogonality is much higher in the MV case thus the introduced bias is also lower [?]. The SNR increases slightly for the MV case listed in the table ?? and it provides much better results for the parameter estimation step. The closely spaced peaks are easier to be estimated via HTLS in case of the high SNR for the signal. Since the gap between the signal and the noise singular values is smaller in the MV case, the estimated parameters preserve better accuracy [?]

4.2 Cadzow vs Multi-Channel Cadzow

The very main difference between Cadzow and Multichannel Cadzow is that correlation between the channels can be fully exploited thereby a significant improvement of SNR has been observed in this case[?] as it is also testified in table ???. This is an important feature for multichannel data which enables the estimation of the common dynamics among the systems. Common dynamic among multichannel's means the same signal interfere throughout the voxels which is superimposed at different location in the brain at different phase and amplitude. This method is also estimated to be performed quite good at low spatial correlation of the NMR signal[?].

In this specific case the signal coming from one voxel will be intervened from the other surrounding voxels. However the scale of the correlation is different depending on the type of tissue which sit on the voxel and the geometrical distance between each voxel. In the Cadzow case this is not taken into consideration therefore the signal is significantly lower.

In this case only one of the surrounding voxels is taken into consideration, meaning that this algorithm is totally blind from the further tissues (neighbouring voxels). Nevertheless it outperforms the traditional Cadzow subspace algorithms.

In multichannel approach, the signal of interest is approximated via a linear combination of the information coming from all the decomposed subspaces of the signal itself together with the other common subspace information coming from the other neighbouring voxels. Therefore, combination of this information will significantly enhance the signal and therefore the unwanted signals are suppressed quite efficiently.

4.3 Cadzow vs Optimized Multi-Channel Cadzow

A further improvement of the MCC is evidenced. As already stated, Cadzow is trying to suppress the noise into a single channel whereas MCCE attempt to provide the best performance possible.

At first the algorithm tries to observe the difference correlation between neighbours voxels along different direction. Whereby it considers only those specific voxels which contribute the most to the common dynamics. Unlike the simplest version of Cadzow, MCCE reveals that the vertically and horizontally voxels due to their proximity to the voxel of interest share much higher mutual information regarding the metabolite.

After decomposition of this signals into different subspaces, the reconstructed signal takes into account the number subspaces where the information is correlated mostly to the voxel of interest. Consequently big amount of consistent information is explored and therefore the enhancement is far better compare to the simple Cadzow.

If the number of neighbourhood increases this means that the number of common dynamics event is also increased. Consequently the SNR of the final signal is testified to be higher. It is also totally not taken into account for the Cadzo algorithm. However, a high number of neighbouring voxels leads to much more heterogeneous tissues compared to the voxel of interest and thus will decay the performance of the MCCE.

5 Multi-channel data

In this study an ultrasound (US) dataset channel data acquired from **MIRC**² has been utilized. The goal is to remove the US artefact and filter out the undesired part of the signal. US probe a part from the noisy contaminated signal introduces some DC level as well as low frequency signal at the onset of the time course. This appear in the US image as noise and limit the usability of this method in the near field. Additionally **wgn** is also superimposed in the signal which needs to be removed. The US probe being used has a bandwidth from 2-7 MHz meaning that anything appearing outside this band is considered to be noise or artefact. In this application EDS is the underlying model to be employed for subspace signal processing. Since the artefact component appear at lower frequencies with significantly higher level compare to the component sitting at the desired band (DB) (2-7 MHz) figure ?? it is critically important to remove this component without affecting the rest of the signal. This approach would enable a much better noise suppression.

Hereby the subspace framework is utilized wherein 28 component are computed. Then the component where their respective frequency sits outside the DB will be deduced from the original signal. The outcome from this is quite on an acceptable range, since the component of the DB sits at high values compare to the rest of the components ???. The original and the artefact removed signal in time domain are plotted in figure ?? and ?? respectively.

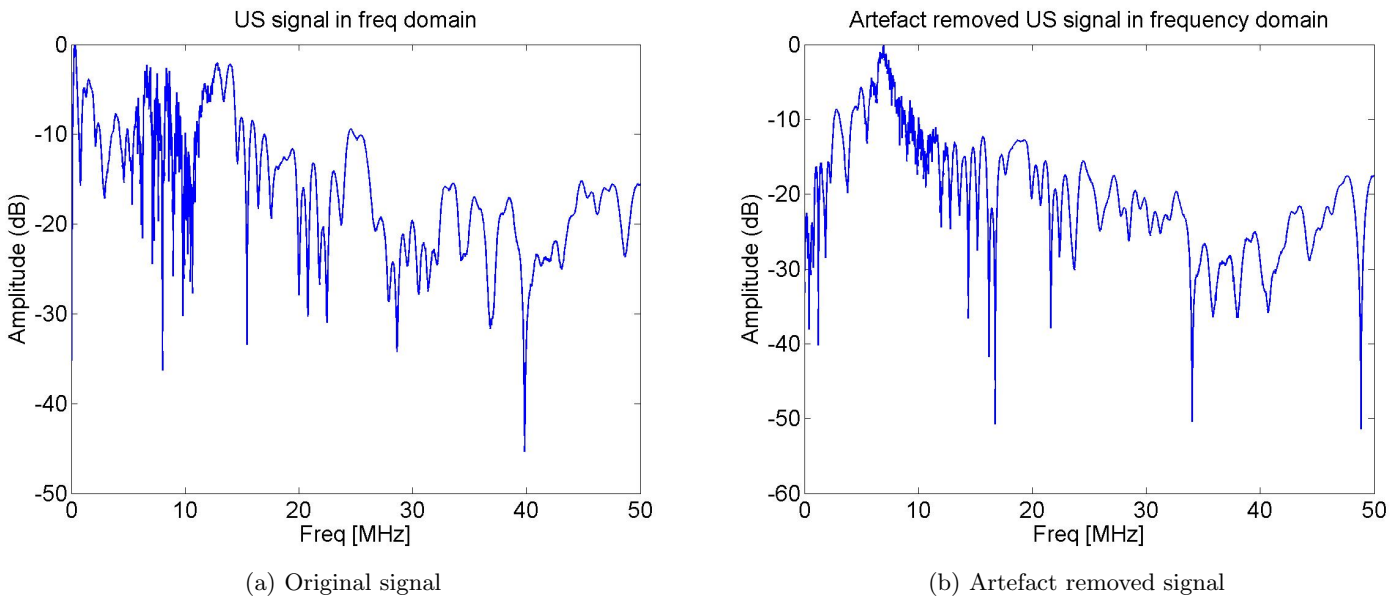


Figure 5.0.1: US signals.

After completing the artefact removal, signal has to be filtered out via subspace signal processing methods. Single channel algorithm Cadzow and minimum variance are alternative solution however their performance would not be the same as compare to the multichannel version of Cadzow. Single channel would not get into account the common dynamics of the neighbouring region of interest being scanned as well as the cross talk between neighbouring ultrasound transducers inside the probe. The only drawback associated with multichannel is its time complexity increases significantly as the number of data-points is much higher. Nevertheless this could be a powerful approach for imaging stationary data via echo whereby an increase in image resolution could be achieved.

Since subspace signal processing is a parametric method, component number of the decomposition is the only input required for this underlying model. In this case, 28 components are chosen to be sufficient number since a higher value would not yield significantly better outcome, given the time complexity would increases dramatically.

Multichannel version would thereby overcome both this obstacles and the outperform both Cadzow and minimum variance. The filtered signal in frequency domain are overlapped in figure ?? where their respective time domain time course could be found in figure ??,??,??. In figure ?? are the normalised spectrum where at first glance the filtering method suppresses the undesired spectrum down to -20 dB whereby the DB is totally untouched.

Table 3: SNR evaluation for different methods

	OriginalSignal	Cadzow	MV	MCC
SNR	-5.2161	10.3109	10.3109	10.7620

In order to testify the performance of these filtering method the SNR has been computed via equation ?? in the frequency domain. The numerator is the variance of the DB whereas the denominator is the variance of all the components outside the DB. In table ?? are the SNR listed where it could be increase of signal quality where the multichannel case outperforms the rest of the methods. Quite important to mention that high dynamics of the signal (very high frequency components) being filtered out via multichannel is visually notable in figure ??.

²Medical Imaging Research Center UZ Leuven

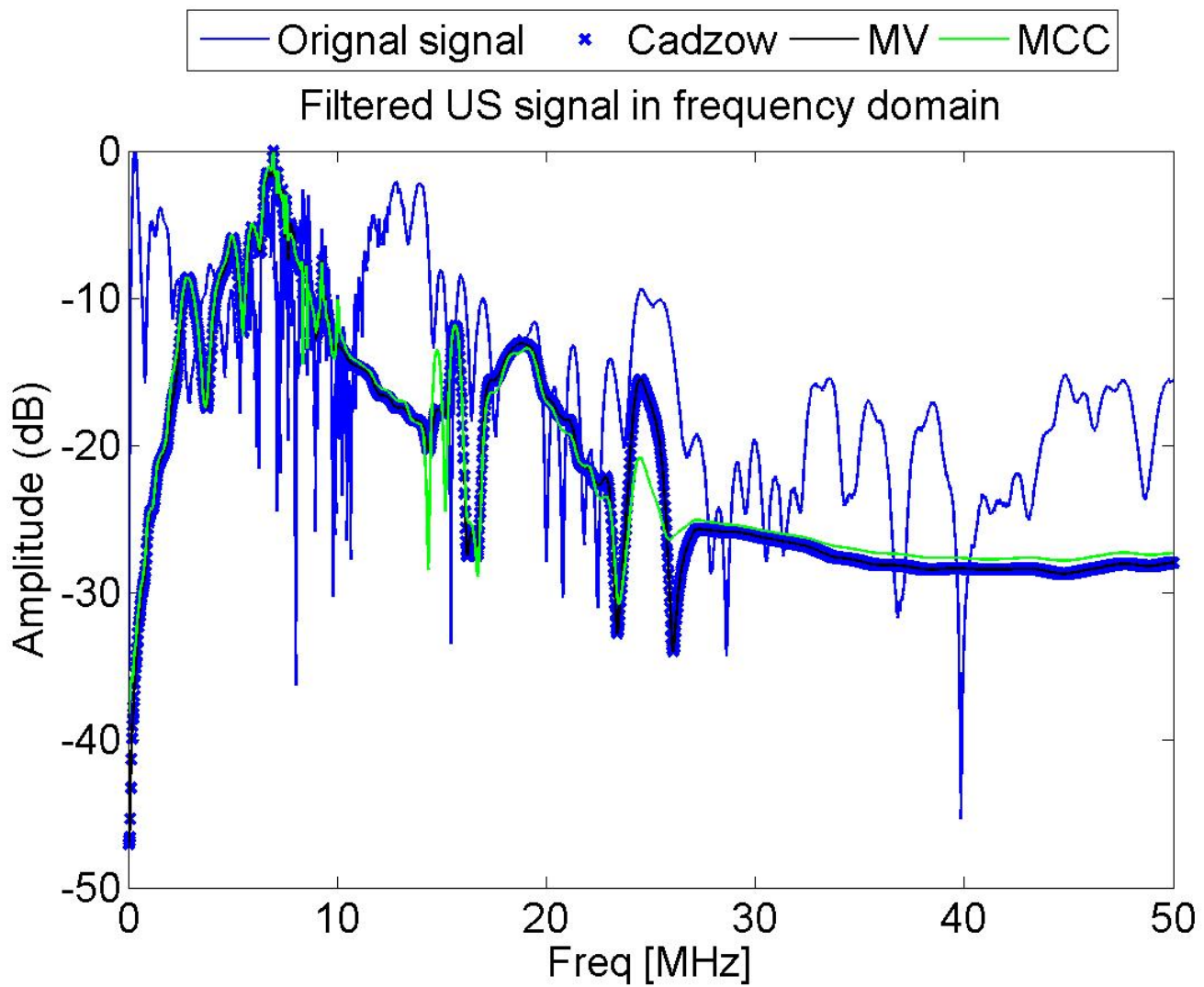
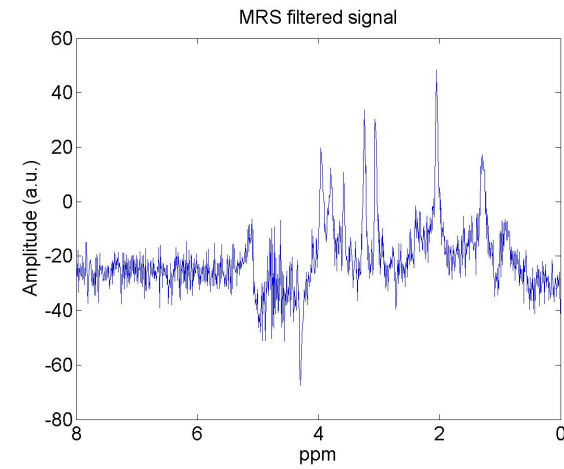
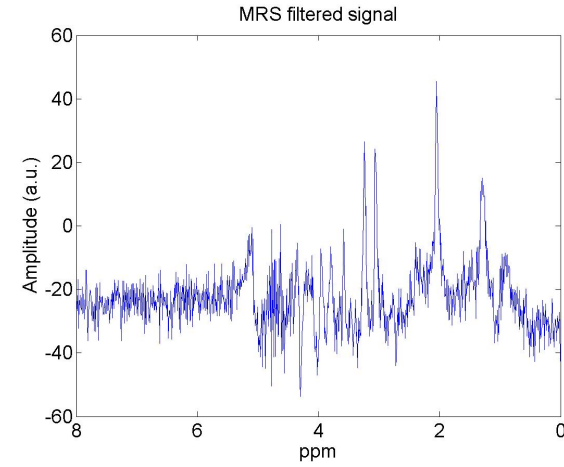
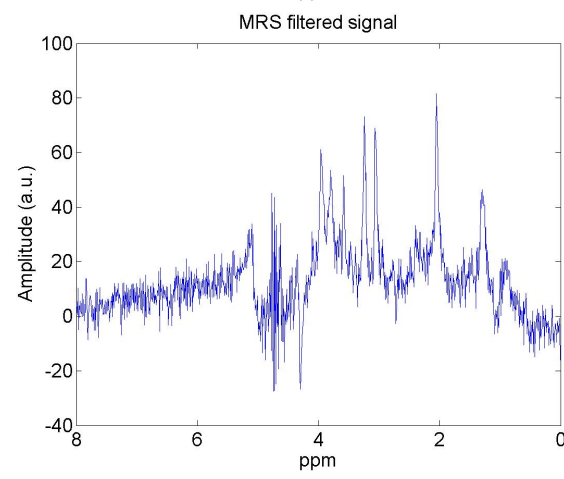
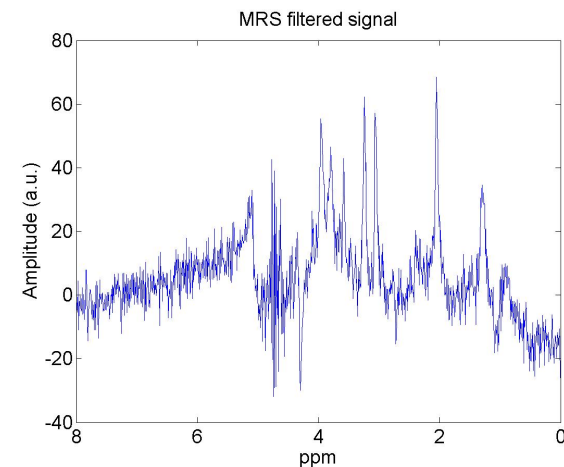
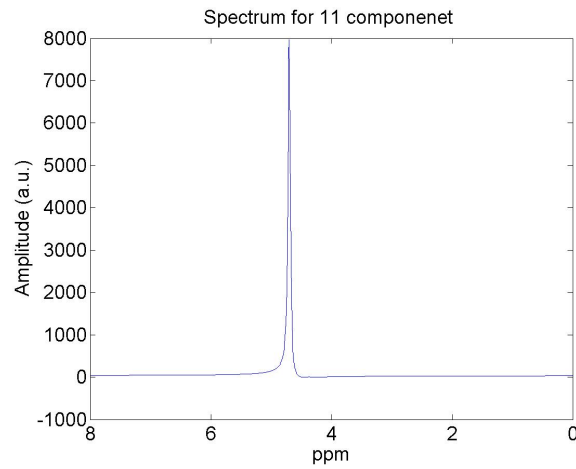
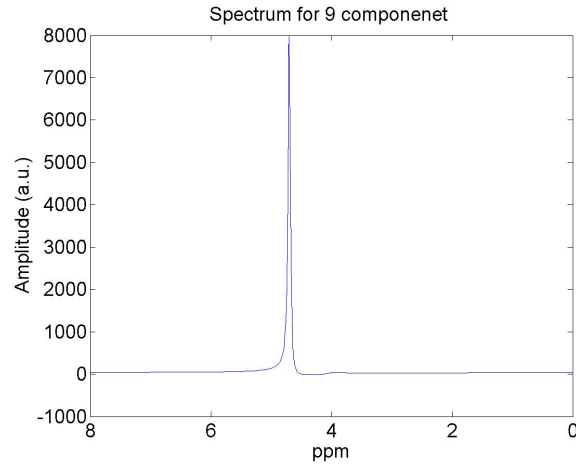
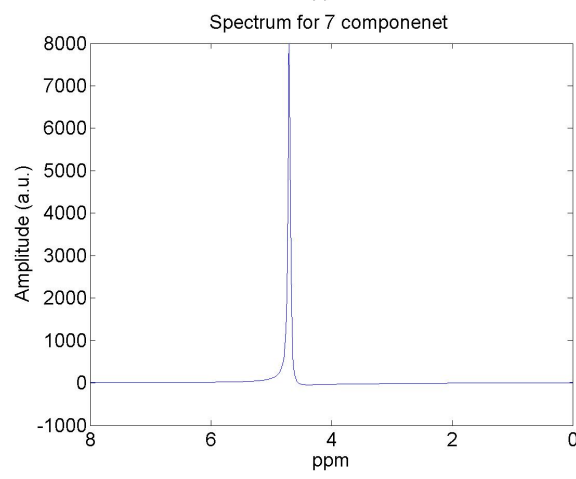
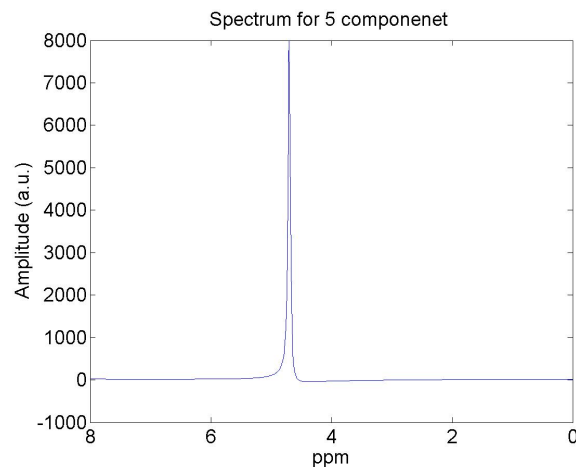
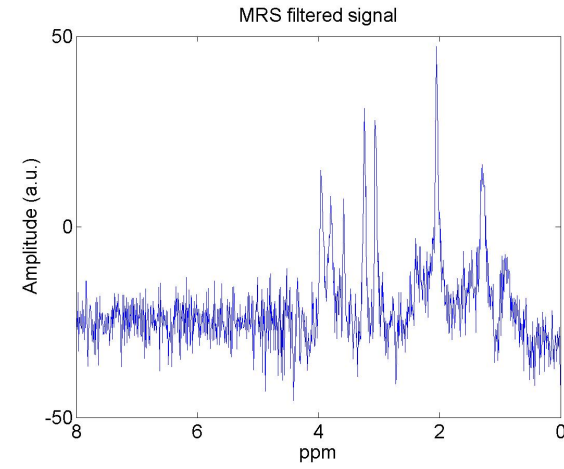
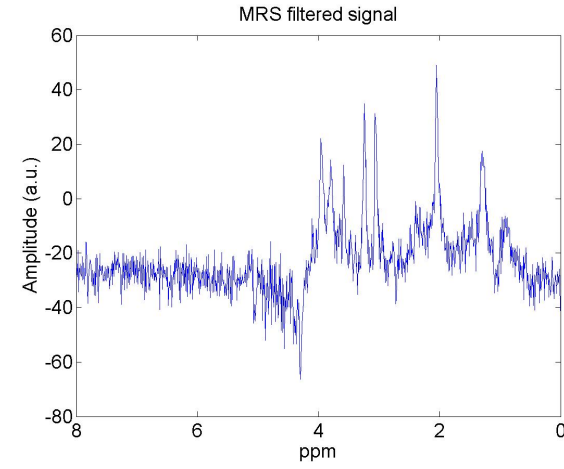
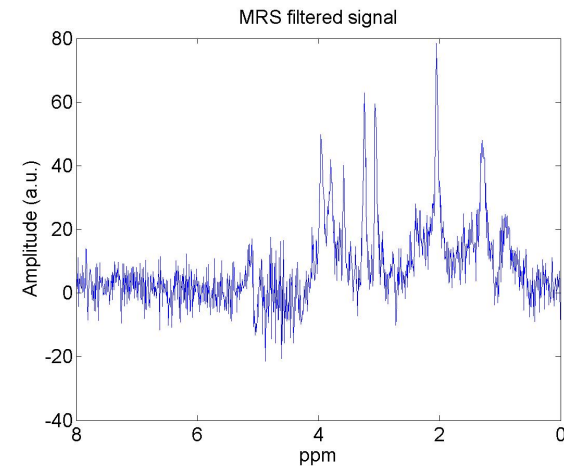
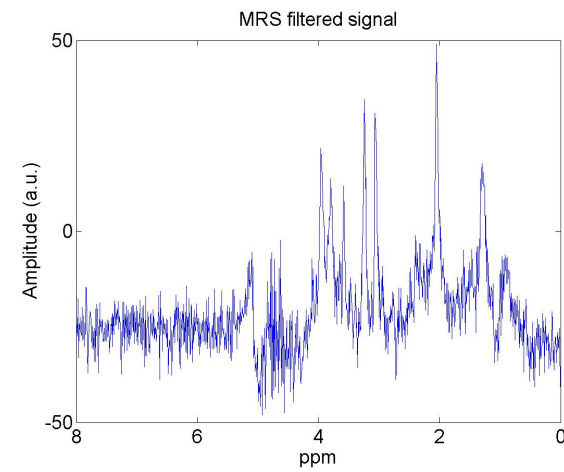
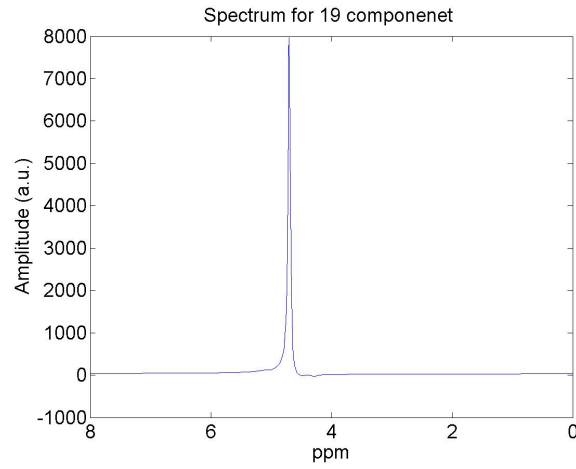
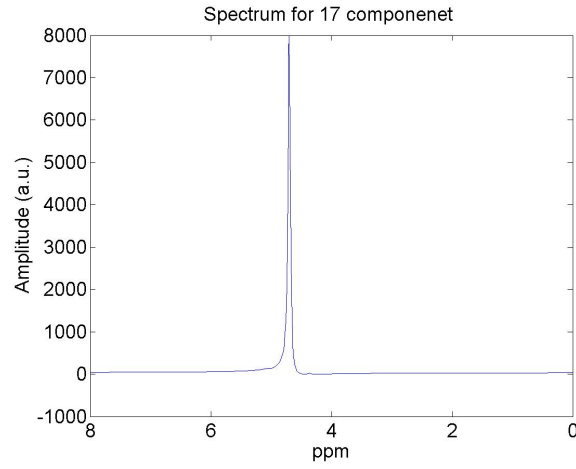
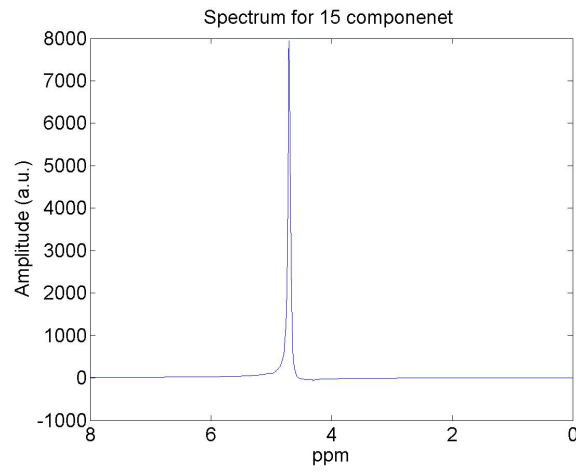
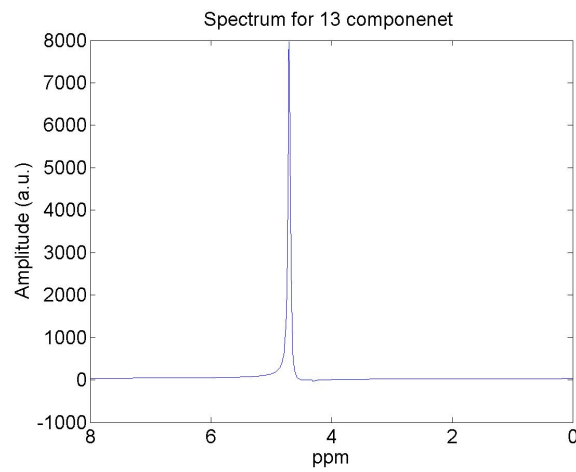


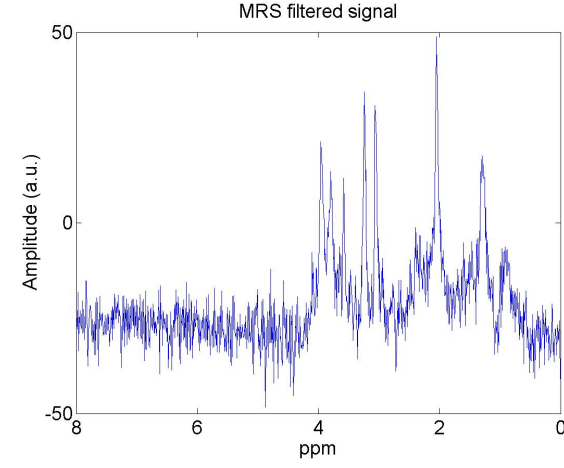
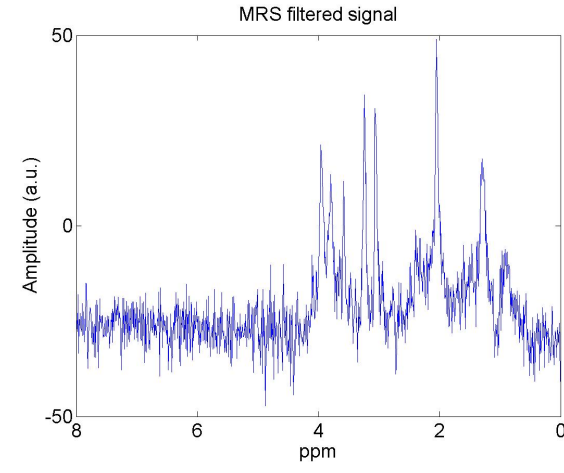
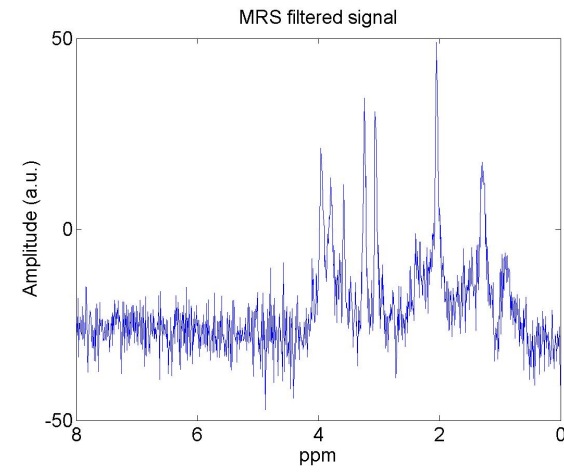
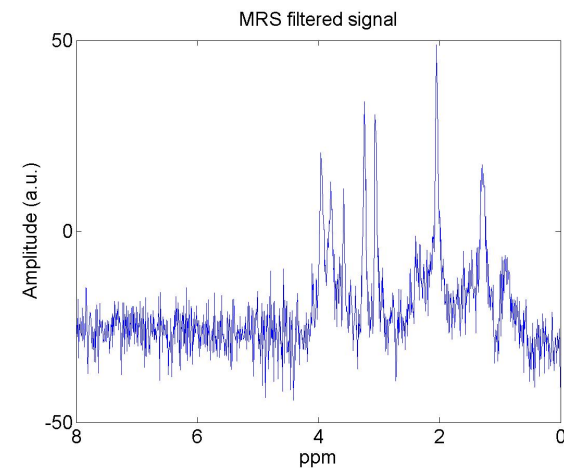
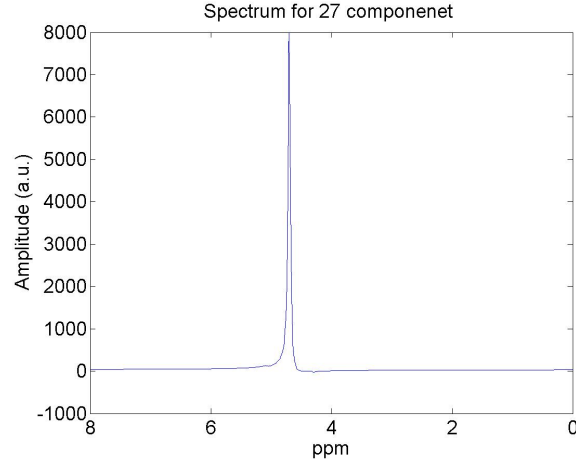
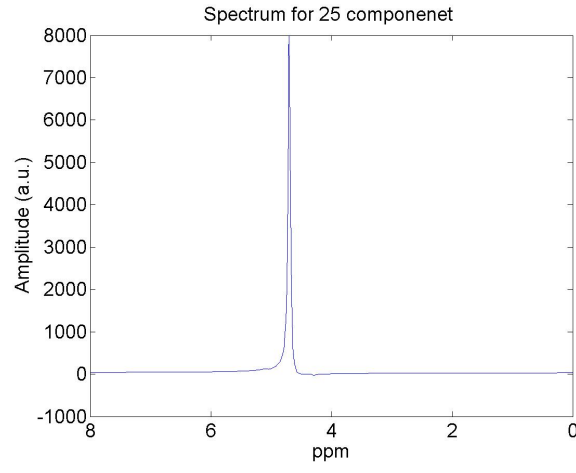
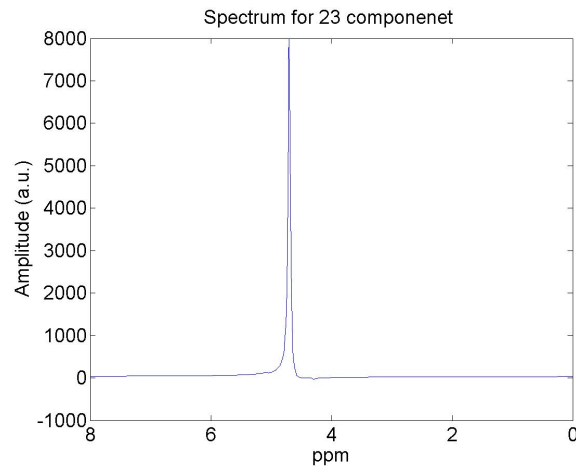
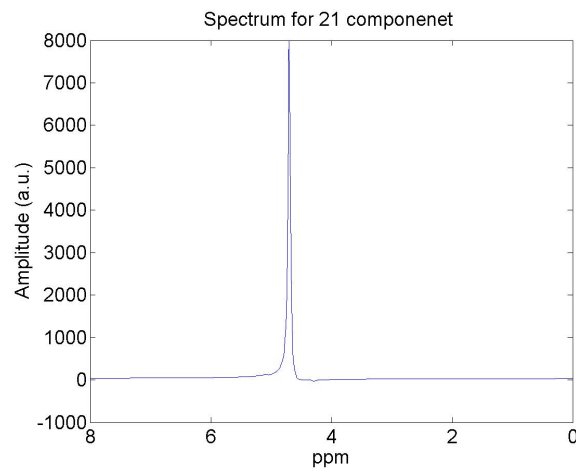
Figure 5.0.2: US filtered signal

A Additional figure

A.1 Outcome for different model order







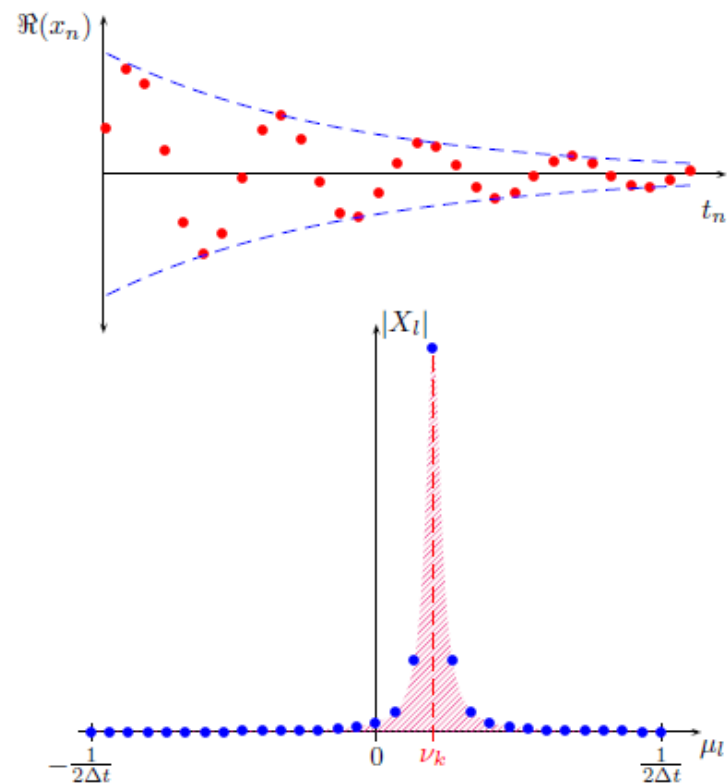
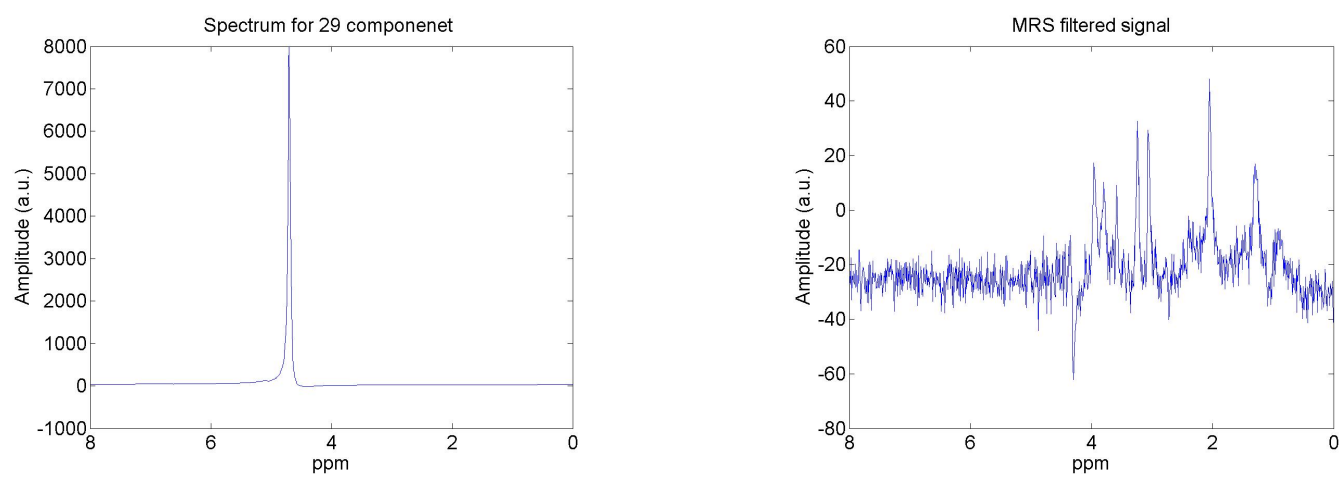


Figure A.1.5: Exponentially damping sinusoidal underlying model

B Parameter estimation

B.1 Residue signal after reconstruction

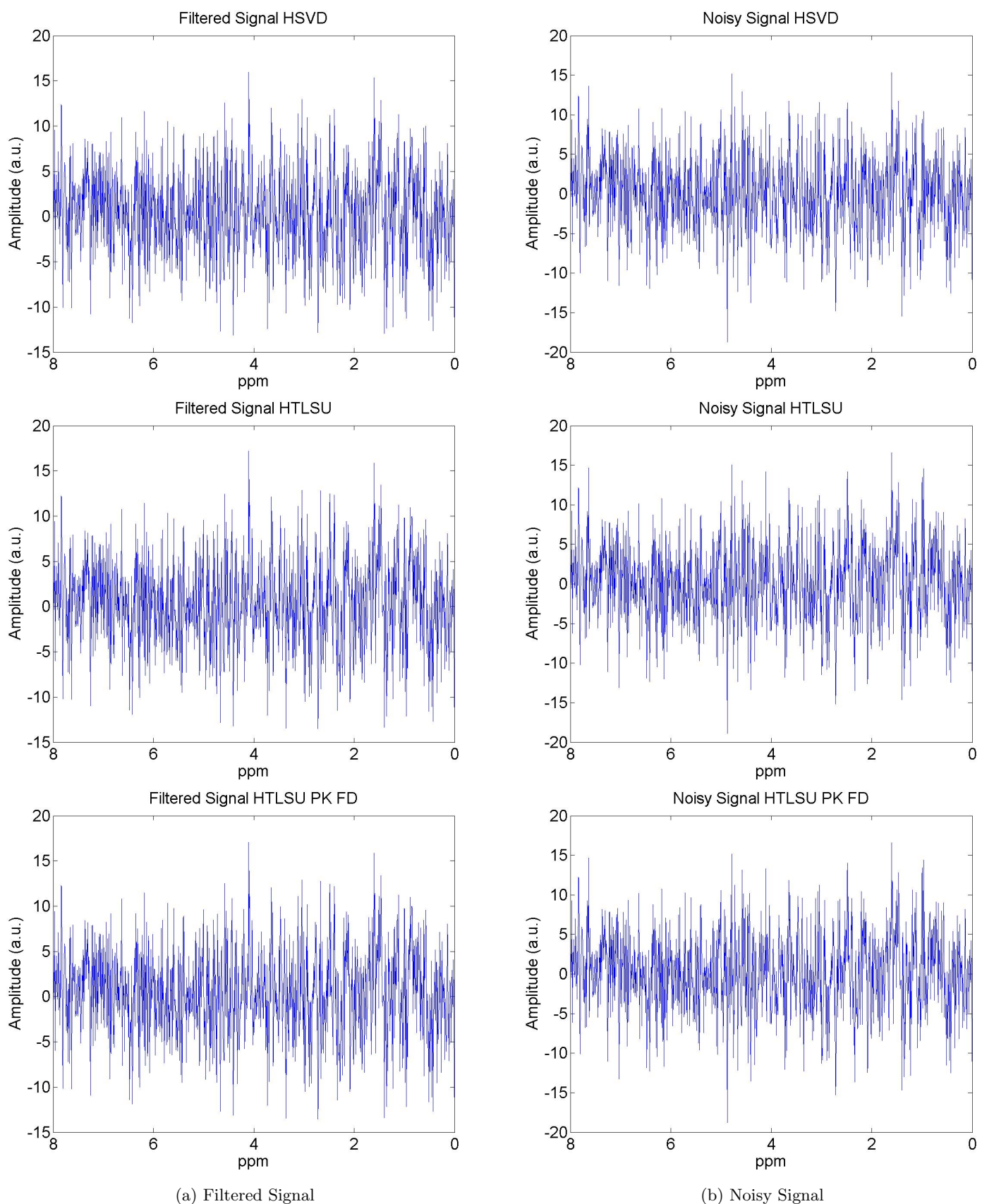


Figure B.1.1: Residue Signal

B.2 Individual component for each method

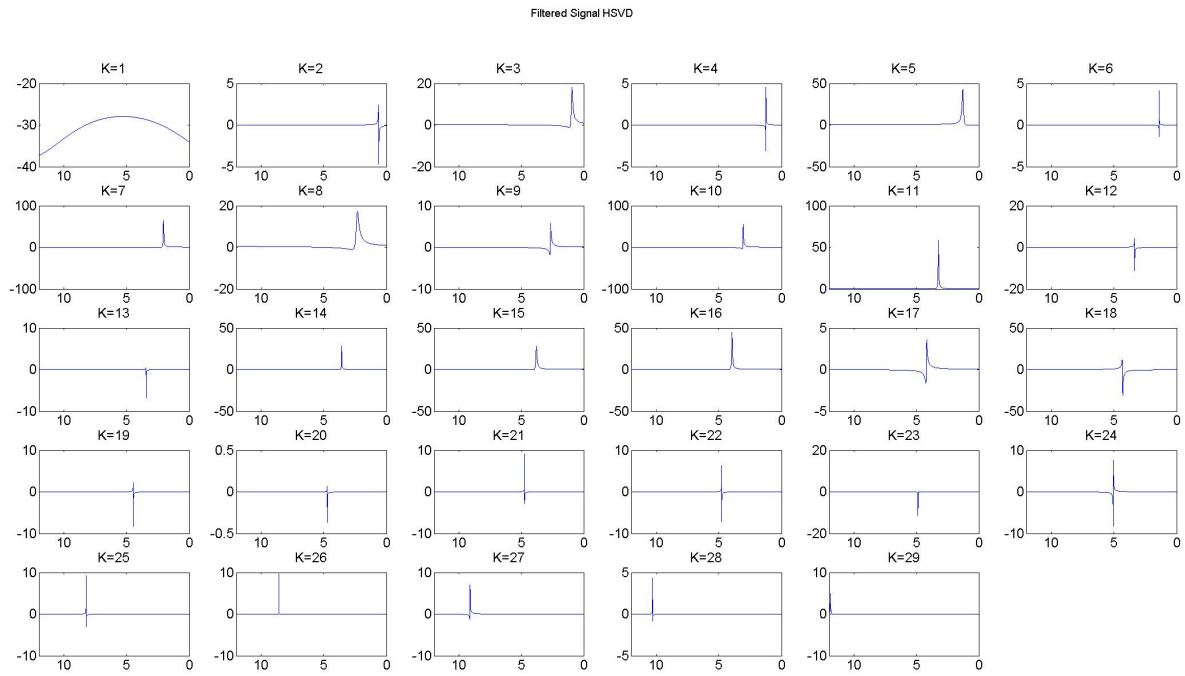


Figure B.2.1: Individual component

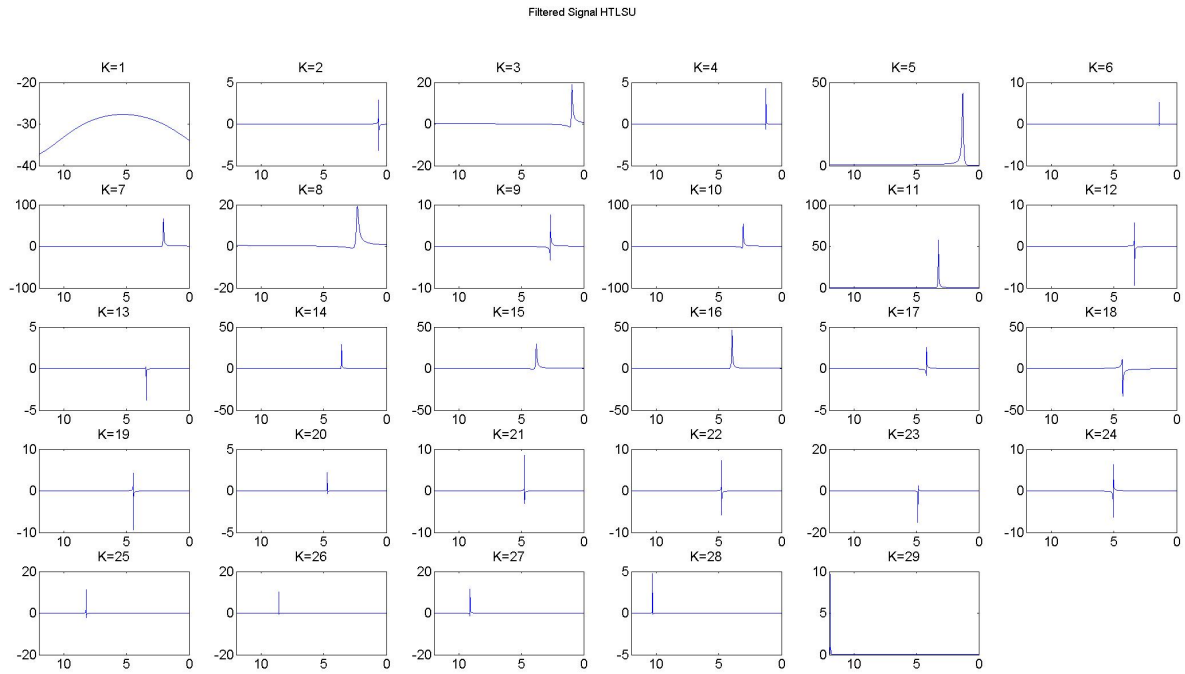


Figure B.2.2: Individual component

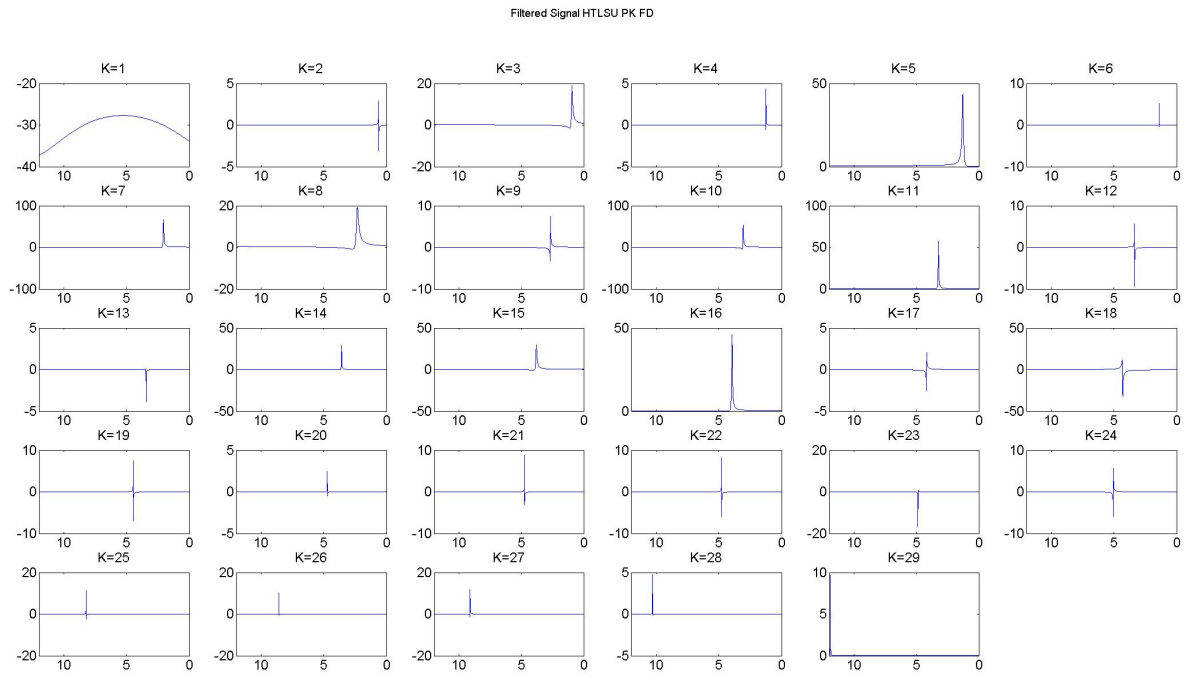


Figure B.2.3: Individual component

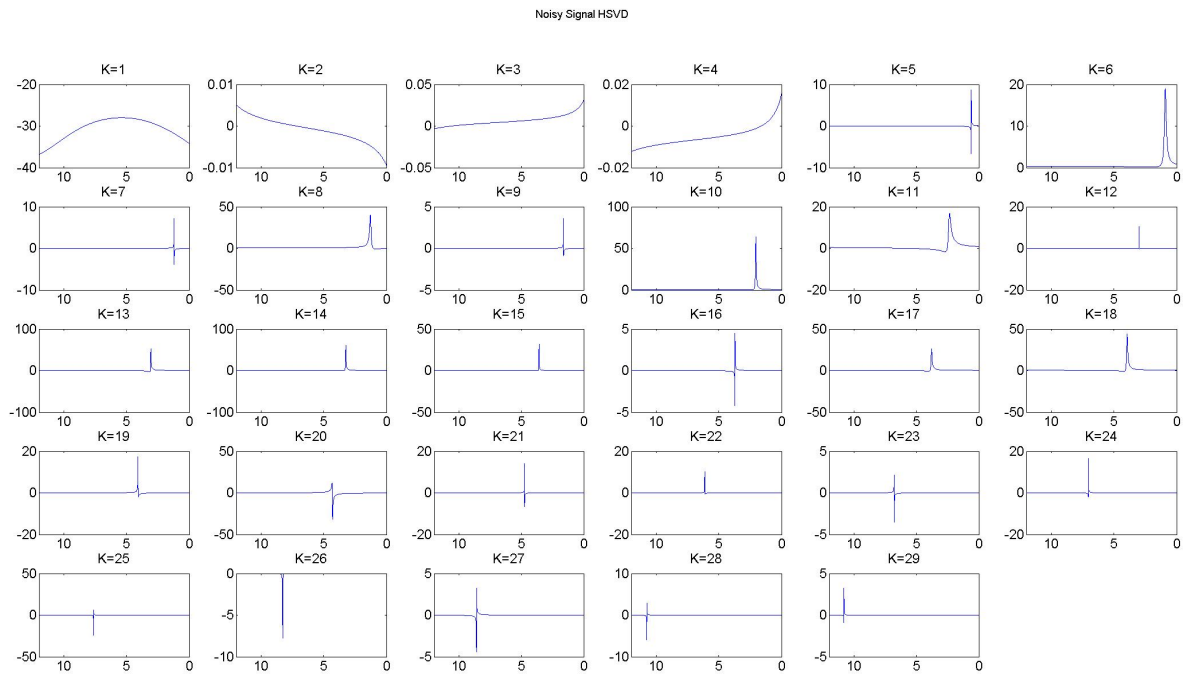


Figure B.2.4: Individual component

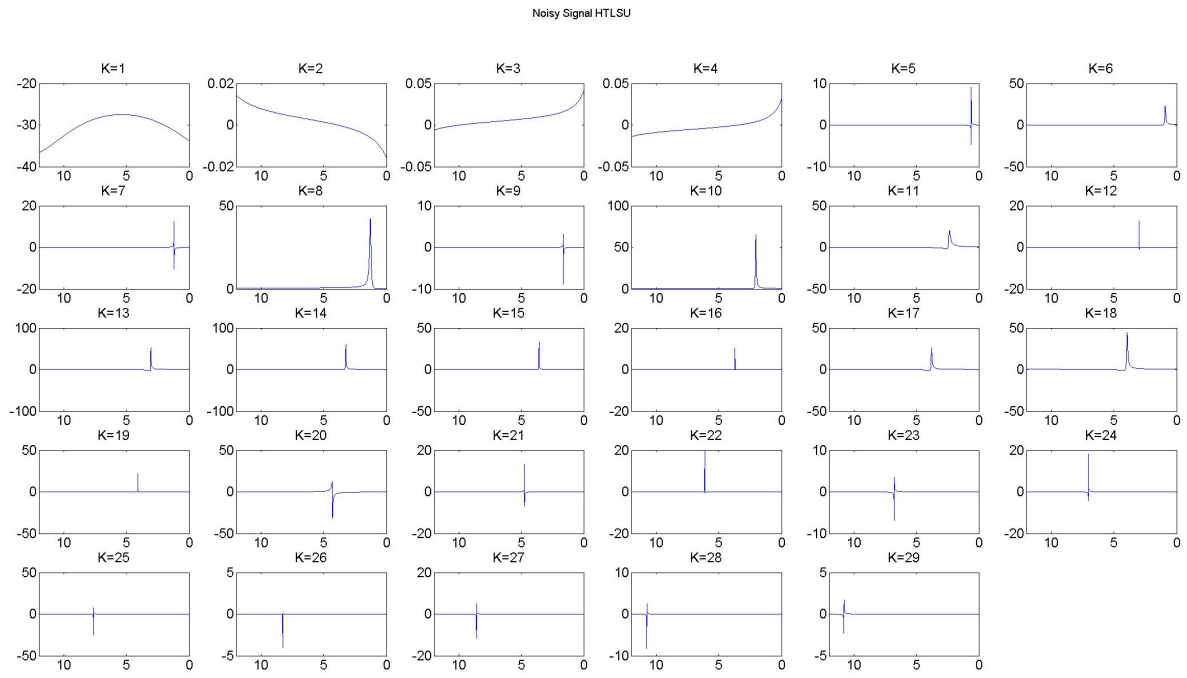


Figure B.2.5: Individual component

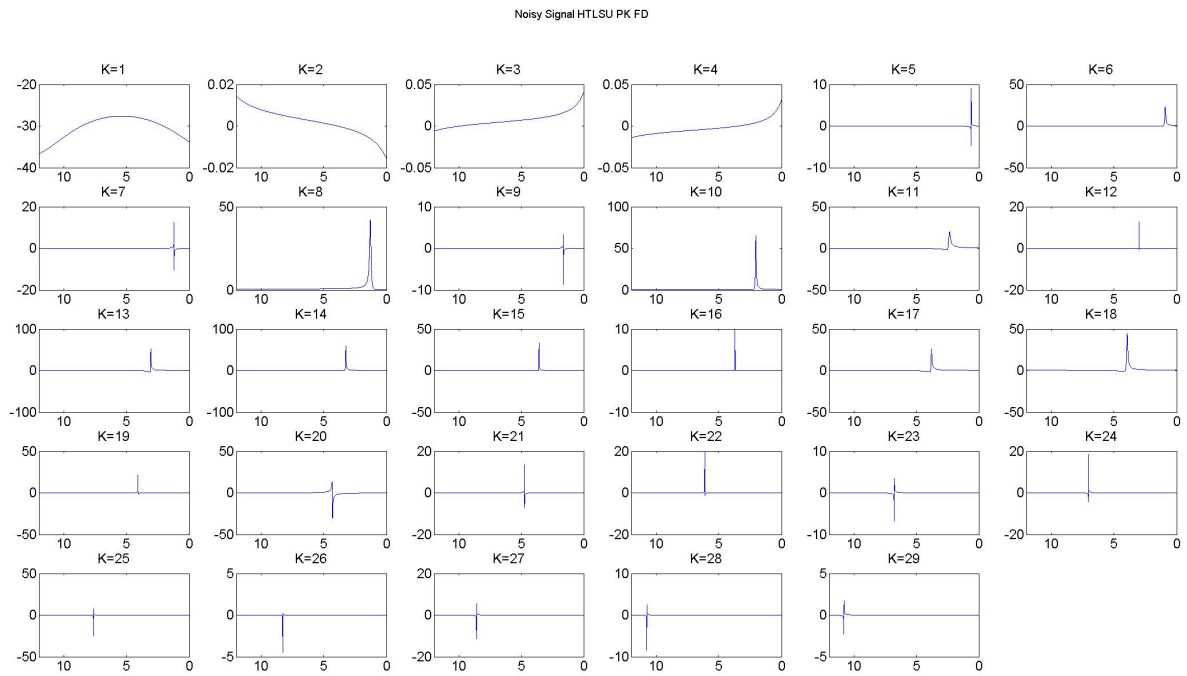


Figure B.2.6: Individual component

B.3 Parameter estimation

Table 4: Frequency estimation **Hz**

<i>Compo</i>	<i>HSVD</i>	<i>HTLS</i>	<i>HTLSPKF</i>	<i>HSVD</i>	<i>HTLS</i>	<i>HTLSPKF</i>
<i>K</i>	<i>Puresignal</i>	<i>Puresignal</i>	<i>Puresignal</i>	<i>Noisysignal</i>	<i>Noisysignal</i>	<i>Noisysignal</i>
1	-9.626694e - 01	-9.627053e - 01	-9.632874e - 01	-9.643108e - 01	-9.646079e - 01	-9.657969e - 01
2	-5.210719e - 01	-5.210816e - 01	-5.210972e - 01	-8.916373e - 01	-8.916375e - 01	-8.916414e - 01
3	-4.781416e - 01	-4.781036e - 01	-4.780446e - 01	-8.546871e - 01	-8.547197e - 01	-8.546967e - 01
4	-4.422369e - 01	-4.422527e - 01	-4.422585e - 01	-4.720727e - 01	-4.728470e - 01	-4.729502e - 01
5	-4.379690e - 01	-4.374794e - 01	-4.374718e - 01	-4.357315e - 01	-4.345490e - 01	-4.356127e - 01
6	-4.227945e - 01	-4.228081e - 01	-4.228097e - 01	-4.194509e - 01	-4.190631e - 01	-4.348804e - 01
7	-3.384021e - 01	-3.382304e - 01	-3.382298e - 01	-3.872168e - 01	-3.869570e - 01	-3.872107e - 01
8	-3.001907e - 01	-3.010434e - 01	-3.009310e - 01	-3.391953e - 01	-3.389534e - 01	-3.388372e - 01
9	-2.602797e - 01	-2.602926e - 01	-2.603064e - 01	-2.486242e - 01	-2.509898e - 01	-2.510541e - 01
10	-2.085534e - 01	-2.085383e - 01	-2.085309e - 01	-2.427150e - 01	-2.421326e - 01	-2.422754e - 01
11	-1.865442e - 01	-1.865024e - 01	-1.864889e - 01	-2.084503e - 01	-2.084633e - 01	-2.084461e - 01
12	-1.714265e - 01	-1.714112e - 01	-1.714053e - 01	-1.867638e - 01	-1.861217e - 01	-1.861817e - 01
13	-1.625687e - 01	-1.625511e - 01	-1.625620e - 01	-1.799649e - 01	-1.805312e - 01	-1.779077e - 01
14	-1.427146e - 01	-1.427270e - 01	-1.426968e - 01	-1.426712e - 01	-1.425187e - 01	-1.423551e - 01
15	-1.147937e - 01	-1.145830e - 01	-1.143345e - 01	-1.145581e - 01	-1.142624e - 01	-1.140365e - 01
16	-9.475129e - 02	-9.482305e - 02	-9.483758e - 02	-9.475876e - 02	-9.473963e - 02	-9.449700e - 02
17	-6.431392e - 02	-6.429654e - 02	-6.533485e - 02	-6.249926e - 02	-6.246462e - 02	-6.269987e - 02
18	-4.951058e - 02	-4.947576e - 02	-4.938121e - 02	-4.977515e - 02	-4.967451e - 02	-4.973399e - 02
19	-2.991272e - 02	-2.987616e - 02	-2.970620e - 02	4.194325e - 03	4.026682e - 03	2.109625e - 03
20	2.533344e - 03	2.537606e - 03	2.552912e - 03	9.570241e - 03	9.713978e - 03	9.034079e - 03
21	5.667499e - 03	5.666552e - 03	5.670188e - 03	3.698128e - 02	3.709557e - 02	3.555008e - 02
22	1.024378e - 02	1.023374e - 02	1.026498e - 02	6.296498e - 02	6.313773e - 02	6.295143e - 02
23	2.214120e - 02	2.215857e - 02	2.224271e - 02	1.294108e - 01	1.294192e - 01	1.294667e - 01
24	4.583127e - 02	4.582998e - 02	4.587339e - 02	3.875065e - 01	3.875046e - 01	3.875132e - 01
25	4.509366e - 01	4.509352e - 01	4.509335e - 01	5.636453e - 01	5.635277e - 01	5.642236e - 01
26	4.960399e - 01	4.960346e - 01	4.960326e - 01	5.772231e - 01	5.772391e - 01	5.772354e - 01
27	5.638691e - 01	5.638245e - 01	5.638178e - 01	7.155686e - 01	7.155764e - 01	7.155715e - 01
28	7.165950e - 01	7.165930e - 01	7.165925e - 01	7.504817e - 01	7.504801e - 01	7.504793e - 01
29	9.176872e - 01	9.176687e - 01	9.176812e - 01	9.176020e - 01	9.175729e - 01	9.175740e - 01

Table 5: Damping estimation **Hz**

<i>Compo</i>	<i>HSVD</i>	<i>HTLS</i>	<i>HTLSPKF</i>	<i>HSVD</i>	<i>HTLS</i>	<i>HTLSPKF</i>
<i>K</i>	<i>Puresignal</i>	<i>Puresignal</i>	<i>Puresignal</i>	<i>Noisysignal</i>	<i>Noisysignal</i>	<i>Noisysignal</i>
1	3.773161e + 00	3.724575e + 00	3.732163e + 00	3.840225e + 00	3.739478e + 00	3.701133e + 00
2	4.733518e - 03	1.774721e - 03	1.761356e - 03	-1.101013e - 04	-1.072161e - 03	-1.069531e - 03
3	5.049520e - 02	4.016098e - 02	4.014253e - 02	3.684974e - 03	2.036576e - 03	2.073344e - 03
4	1.086866e - 03	-2.966453e - 05	-2.470847e - 05	3.516539e - 02	2.460751e - 02	2.598903e - 02
5	5.267441e - 02	5.217549e - 02	5.214805e - 02	4.905126e - 02	5.177228e - 02	2.822807e - 03
6	6.320581e - 04	1.038774e - 04	1.037390e - 04	1.448997e - 01	3.011524e - 02	6.852561e - 02
7	2.518961e - 02	2.593446e - 02	2.585060e - 02	1.866042e - 03	-7.205628e - 04	-1.251409e - 03
8	1.035565e - 01	8.228955e - 02	8.321119e - 02	3.425268e - 02	3.540646e - 02	3.471359e - 02
9	2.153725e - 02	6.872616e - 03	6.713500e - 03	1.587209e - 02	5.469765e - 03	6.300096e - 03
10	1.647647e - 02	1.615665e - 02	1.616265e - 02	3.491172e - 02	7.573407e - 03	8.066691e - 03
11	2.143422e - 02	2.100473e - 02	2.101694e - 02	1.490174e - 02	1.479340e - 02	1.461361e - 02
12	4.007320e - 03	2.044200e - 03	2.020617e - 03	1.753937e - 02	1.572056e - 02	1.667447e - 02
13	1.862180e - 03	9.982267e - 04	9.853592e - 04	5.748950e - 02	1.106466e - 02	9.796166e - 03
14	1.307169e - 02	1.224638e - 02	1.218924e - 02	2.698117e - 02	1.743363e - 02	1.590902e - 02
15	4.179071e - 02	3.804346e - 02	3.830741e - 02	3.085321e - 02	2.656422e - 02	2.514633e - 02
16	2.860605e - 02	2.887068e - 02	2.938310e - 02	2.997883e - 02	2.956320e - 02	3.025620e - 02
17	2.612756e - 02	6.290727e - 03	6.728312e - 03	5.976457e - 03	1.279564e - 03	2.267936e - 03
18	1.457910e - 02	1.332156e - 02	1.310132e - 02	1.285614e - 02	1.122959e - 02	1.035164e - 02
19	2.305775e - 03	1.206624e - 03	7.268034e - 04	8.015718e - 03	1.229016e - 03	2.077616e - 03
20	4.699147e - 04	-7.214790e - 04	-7.322746e - 04	4.542459e - 03	-9.124793e - 04	-7.161473e - 04
21	-1.843201e - 04	-3.503979e - 04	-3.736536e - 04	1.419182e - 02	1.818500e - 03	2.685072e - 03
22	3.236792e - 04	-7.374764e - 04	-7.242577e - 04	1.064620e - 02	2.300070e - 04	-3.540073e - 06
23	3.674760e - 03	1.378930e - 03	1.530632e - 03	3.869246e - 03	2.156197e - 03	2.189245e - 03
24	3.091770e - 03	1.812516e - 03	1.742459e - 03	-3.549396e - 04	-9.279296e - 04	-9.266635e - 04
25	1.629041e - 04	-1.083549e - 03	-1.079502e - 03	2.469717e - 02	4.917533e - 03	4.585493e - 03
26	1.001152e - 03	6.496526e - 06	1.208454e - 05	1.986701e - 03	-1.648039e - 03	-1.644252e - 03
27	6.515594e - 03	2.565443e - 03	2.590122e - 03	1.211370e - 03	-1.176761e - 03	-1.171978e - 03
28	-3.503161e - 04	-1.629671e - 03	-1.627272e - 03	-2.353914e - 04	-6.292998e - 04	-6.276378e - 04
29	1.398110e - 02	4.705212e - 03	4.685577e - 03	3.760964e - 03	2.729768e - 03	2.787495e - 03

Table 6: Amplitude estimation $a.u$

<i>Compo</i>	<i>HSVD</i>	<i>HTLS</i>	<i>HTLSPKF D</i>	<i>HSVD</i>	<i>HTLS</i>	<i>HTLSPKF D</i>
<i>K</i>	<i>Puresignal</i>	<i>Puresignal</i>	<i>Puresignal</i>	<i>Noisysignal</i>	<i>Noisysignal</i>	<i>Noisysignal</i>
1	$3.231920e + 01$	$3.215251e + 01$	$3.215701e + 01$	$3.228869e + 01$	$3.174675e + 01$	$3.163893e + 01$
2	$1.747603e - 02$	$5.492805e - 03$	$5.588675e - 03$	$6.769893e - 03$	$4.298463e - 03$	$4.320191e - 03$
3	$4.852758e - 01$	$4.106912e - 01$	$4.088752e - 01$	$1.589341e - 02$	$1.479805e - 02$	$1.484834e - 02$
4	$9.726507e - 03$	$5.378445e - 03$	$5.426258e - 03$	$4.301316e - 01$	$2.771124e - 01$	$2.801833e - 01$
5	$1.141549e + 00$	$1.136913e + 00$	$1.135292e + 00$	$1.116191e + 00$	$1.356550e + 00$	$1.105734e - 02$
6	$7.433318e - 03$	$5.460629e - 03$	$5.453569e - 03$	$1.509883e + 00$	$3.436951e - 01$	$1.398523e + 00$
7	$8.230386e - 01$	$8.654992e - 01$	$8.622624e - 01$	$1.658740e - 02$	$6.177020e - 03$	$5.424569e - 03$
8	$9.485149e - 01$	$8.327856e - 01$	$8.382427e - 01$	$1.056976e + 00$	$1.148234e + 00$	$1.136158e + 00$
9	$8.237458e - 02$	$3.890474e - 02$	$3.781552e - 02$	$1.795637e - 01$	$3.890524e - 02$	$4.707427e - 02$
10	$4.866146e - 01$	$4.733832e - 01$	$4.725199e - 01$	$3.618841e - 01$	$6.448762e - 02$	$7.100071e - 02$
11	$6.252968e - 01$	$6.069694e - 01$	$6.059894e - 01$	$4.314890e - 01$	$4.206534e - 01$	$4.189275e - 01$
12	$3.107758e - 02$	$1.550966e - 02$	$1.531024e - 02$	$4.646532e - 01$	$4.666732e - 01$	$4.888759e - 01$
13	$1.533534e - 02$	$1.149540e - 02$	$1.141014e - 02$	$2.836226e - 01$	$5.003206e - 02$	$4.123508e - 02$
14	$1.872614e - 01$	$1.816507e - 01$	$1.798042e - 01$	$2.871985e - 01$	$2.008714e - 01$	$1.865485e - 01$
15	$5.997481e - 01$	$5.724793e - 01$	$5.758834e - 01$	$4.882085e - 01$	$4.336632e - 01$	$4.110433e - 01$
16	$6.432660e - 01$	$6.738184e - 01$	$6.831276e - 01$	$7.159821e - 01$	$7.315288e - 01$	$7.514699e - 01$
17	$6.861603e - 02$	$1.182744e - 02$	$1.551450e - 02$	$2.584987e - 02$	$2.193267e - 02$	$2.368334e - 02$
18	$3.161367e - 01$	$2.955947e - 01$	$2.896821e - 01$	$2.703530e - 01$	$2.428253e - 01$	$2.320671e - 01$
19	$1.275428e - 02$	$1.045658e - 02$	$8.976775e - 03$	$2.275399e - 02$	$1.064569e - 02$	$7.820888e - 03$
20	$1.361250e - 03$	$1.679376e - 03$	$1.659680e - 03$	$4.520306e - 03$	$1.651962e - 03$	$1.551731e - 03$
21	$6.561102e - 03$	$5.937452e - 03$	$5.908705e - 03$	$5.309079e - 02$	$1.659452e - 02$	$8.889503e - 03$
22	$6.525969e - 03$	$4.033061e - 03$	$4.212808e - 03$	$2.057176e - 02$	$3.088502e - 03$	$2.770173e - 03$
23	$2.464802e - 02$	$1.705823e - 02$	$1.838809e - 02$	$2.752925e - 02$	$2.209700e - 02$	$2.263805e - 02$
24	$3.250744e - 02$	$2.360855e - 02$	$2.338776e - 02$	$9.377389e - 03$	$6.810893e - 03$	$6.796702e - 03$
25	$5.716683e - 03$	$3.390915e - 03$	$3.401278e - 03$	$6.106855e - 02$	$2.681010e - 02$	$3.871995e - 02$
26	$7.743065e - 03$	$5.063343e - 03$	$5.091904e - 03$	$9.586182e - 03$	$3.937391e - 03$	$3.933401e - 03$
27	$2.709586e - 02$	$1.891033e - 02$	$1.901267e - 02$	$1.259137e - 02$	$3.726674e - 03$	$3.762564e - 03$
28	$2.375034e - 03$	$1.043778e - 03$	$1.044558e - 03$	$8.235952e - 03$	$6.673623e - 03$	$6.698358e - 03$
29	$3.548228e - 02$	$2.594324e - 02$	$2.580903e - 02$	$4.131973e - 02$	$3.556140e - 02$	$3.613318e - 02$

Table 7: Phase estimation **Deg**

<i>Compo</i>	<i>HSVD</i>	<i>HTLS</i>	<i>HTLSPKF D</i>	<i>HSVD</i>	<i>HTLS</i>	<i>HTLSPKF D</i>
<i>K</i>	<i>Puresignal</i>	<i>Puresignal</i>	<i>Puresignal</i>	<i>Noisysignal</i>	<i>Noisysignal</i>	<i>Noisysignal</i>
1	$1.854297e + 02$	$1.855126e + 02$	$1.854776e + 02$	$1.861644e + 02$	$1.858703e + 02$	$1.856143e + 02$
2	$1.071438e + 02$	$9.009687e + 01$	$8.876656e + 01$	$2.339356e + 02$	$2.323033e + 02$	$2.334573e + 02$
3	$3.292072e + 02$	$3.280838e + 02$	$3.279417e + 02$	$3.035570e + 02$	$2.947017e + 02$	$2.917486e + 02$
4	$2.712672e + 02$	$2.691599e + 02$	$2.702059e + 02$	$2.924563e + 02$	$3.057743e + 02$	$3.041089e + 02$
5	$1.621396e + 01$	$1.266992e + 01$	$1.268822e + 01$	$3.352158e + 02$	$3.522636e + 02$	$2.296875e + 02$
6	$2.825475e + 02$	$2.919768e + 02$	$2.921217e + 02$	$4.239909e + 01$	$7.632898e + 01$	$5.084751e + 00$
7	$3.490280e + 02$	$3.473570e + 02$	$3.473848e + 02$	$7.372607e + 01$	$3.297576e + 02$	$2.778194e + 01$
8	$3.272824e + 02$	$3.323484e + 02$	$3.319914e + 02$	$6.789289e + 00$	$1.331625e + 00$	$2.761059e - 01$
9	$3.017081e + 02$	$2.935312e + 02$	$2.934719e + 02$	$1.210811e + 02$	$1.793190e + 02$	$1.808961e + 02$
10	$3.307392e + 02$	$3.295687e + 02$	$3.294814e + 02$	$2.450368e + 02$	$2.444327e + 02$	$2.466982e + 02$
11	$3.552152e + 02$	$3.535566e + 02$	$3.534231e + 02$	$3.258757e + 02$	$3.260819e + 02$	$3.255966e + 02$
12	$1.160635e + 02$	$1.100493e + 02$	$1.102848e + 02$	$6.967718e - 01$	$3.436192e + 02$	$3.460082e + 02$
13	$1.623208e + 02$	$1.665321e + 02$	$1.678329e + 02$	$2.747103e + 02$	$3.197522e + 02$	$2.821695e + 02$
14	$3.515232e + 02$	$3.513759e + 02$	$3.510095e + 02$	$3.522863e + 02$	$3.494582e + 02$	$3.474588e + 02$
15	$3.450841e + 02$	$3.417462e + 02$	$3.400527e + 02$	$3.419579e + 02$	$3.350393e + 02$	$3.323329e + 02$
16	$3.497366e + 02$	$3.497970e + 02$	$3.503164e + 02$	$3.492208e + 02$	$3.456343e + 02$	$3.429974e + 02$
17	$2.908476e + 02$	$3.042547e + 02$	$2.641960e + 02$	$2.574768e + 02$	$2.558113e + 02$	$2.786321e + 02$
18	$1.163796e + 02$	$1.189893e + 02$	$1.173942e + 02$	$1.200818e + 02$	$1.197000e + 02$	$1.199060e + 02$
19	$1.309618e + 02$	$1.302926e + 02$	$1.046115e + 02$	$3.026529e + 02$	$3.304748e + 02$	$2.946502e + 02$
20	$1.560959e + 02$	$1.373210e + 02$	$1.295619e + 02$	$1.204519e - 01$	$3.272649e + 02$	$1.987259e + 02$
21	$3.477653e + 02$	$3.466513e + 02$	$3.463836e + 02$	$1.050140e + 02$	$1.310617e + 02$	$1.514548e + 02$
22	$1.134641e + 02$	$1.267713e + 02$	$1.179124e + 02$	$2.402425e + 02$	$2.379513e + 02$	$2.982082e + 02$
23	$1.906313e + 02$	$2.027876e + 02$	$1.924162e + 02$	$1.770140e + 01$	$2.022368e + 01$	$1.497470e + 01$
24	$2.594566e + 02$	$2.620409e + 02$	$2.598886e + 02$	$2.645752e + 02$	$2.624114e + 02$	$2.602216e + 02$
25	$6.090596e + 01$	$6.147002e + 01$	$6.184542e + 01$	$2.672111e + 02$	$3.353872e + 02$	$3.044789e + 02$
26	$3.571560e + 02$	$1.714042e + 00$	$1.943702e + 00$	$2.648545e + 02$	$2.534817e + 02$	$2.548917e + 02$
27	$3.138720e + 02$	$3.286467e + 02$	$3.290935e + 02$	$1.615933e + 02$	$1.287889e + 02$	$1.299680e + 02$
28	$7.686866e + 01$	$7.132020e + 01$	$7.135031e + 01$	$3.419844e + 02$	$3.431418e + 02$	$3.434000e + 02$
29	$1.323392e + 01$	$1.467743e + 00$	$4.647444e - 01$	$3.535617e + 02$	$3.566943e + 02$	$3.564176e + 02$

B.4 Number of parameters

Suppose we have the estimation model to be estimated with wgn³ contamination:

$$x[n] = A_0 + A_1 n + wgn = \sum_{K=0} An^k + wgn \quad (\text{B.4.1})$$

We construct the Fisher information matrix in order to define the CR bound for A_1 and A_2 .

$$p(\hat{x}; \hat{A}) = \frac{1}{(2\pi\sigma^2)^{\frac{N}{2}}} \exp \left\{ -\frac{1}{2*\sigma^2} \sum_n (x[n] - \sum_{K=0} An^k)^2 \right\} \quad (\text{B.4.2})$$

$$\log(p(\hat{x}; \hat{A})) = -\frac{N}{2} \log(2\pi\sigma^2) - \left\{ \frac{1}{2*\sigma^2} \sum_n (x[n] - \sum_{K=0} An^k)^2 \right\} \quad (\text{B.4.3})$$

$$\frac{\delta \log(p(\hat{x}; \hat{A}))}{\delta \hat{A}_i} = \frac{1}{2\sigma^2} \sum_n 2(x[n] - \sum_{K=0} An^k) \frac{\delta \sum An}{A_j} = \frac{1}{\sigma^2} \sum_n (x[n] - \sum_{K=0} An^k) n^i \quad (\text{B.4.4})$$

$$\frac{\delta^2 \log(p(\hat{x}; \hat{A}))}{\delta \hat{A}_i \delta \hat{A}_j} = \frac{1}{\sigma^2} \sum_n (n^i - \frac{\delta \sum An^k}{\delta \hat{A}_j}) = \frac{-1}{\sigma^2} \sum_n n^i n^j \implies I(\hat{A}) = I_{ij} = \frac{1}{\sigma^2} \sum_n n^i n^j \quad (\text{B.4.5})$$

Thereby it is concluded that information matrix $I(A_0 A_1)$ is :

$$I = \begin{pmatrix} \sum_n n^0 n^0 & \sum_n n^0 n^{01} \\ \sum_n n^1 n^0 & \sum_n n^1 n^1 \end{pmatrix} = \begin{pmatrix} N & N(N+1)/2 \\ N(N+1)/2 & N(N+1)(2N+1)/6 \end{pmatrix}$$

In case $\sigma = 1, N = 10$:

$$I = \begin{pmatrix} 10 & 55 \\ 55 & 385 \end{pmatrix}$$

Since the CRLB⁴ is the inverse of the information matrix $CRLB = \begin{pmatrix} 0.4667 & -0.0667 \\ -0.0667 & 0.121 \end{pmatrix}$

Therefore

$$Var(\hat{A}_0) \geq 0.4667 = CRLB_{\hat{A}_0} \quad (\text{B.4.6})$$

and

$$Var(\hat{A}_1) \geq 0.4667 = CRLB_{\hat{A}_1} \quad (\text{B.4.7})$$

However if A_1 is known, then

$$I(A_0) = \frac{1}{\sigma^2} [\sum_n n^0 n^0] \quad (\text{B.4.8})$$

and for $\sigma = 1, N = 10$ $I(A_0) = 10$ and

$$Var(\hat{A}_0) \geq 0.4667 = CRLB_{\hat{A}_0}, \quad (\text{B.4.9})$$

Hence, knowing the value of A_1 , A_0 can be estimated with less certainty. This is because $CRLB(A_1, A_0)$ is not diagonal, meaning there is a non-zero mutual uncertainty in the values of A_1 , A_0 . Consequently, knowing A_1 decreases the uncertainty in A_0 . CRLB increases consistently if the number of parameters to be estimated increases and decreases always information is provided.

³White Gaussian Noise

⁴CRLB=Cramer-Rao Lower Bound

B.5 Revoming the known part in the data

The water filtered signal is restructured into a Hankel Matrix LxM

$$X = \begin{pmatrix} x_0 & x_1 & \cdots & x_m \\ x_1 & x_2 & \cdots & \\ \vdots & \vdots & \ddots & \vdots \\ x_{L-1} & \vdots & \cdots & x_{N-1} \end{pmatrix}$$

Since the date is noise free the the matrix X has a Vandermonde decomposition of the form $X = SCT^T$ where

$$S = \begin{pmatrix} 1 & 1 & \cdots & 1 \\ Z_1^1 & Z_2^1 & \cdots & Z^1 \\ \vdots & \vdots & \ddots & \vdots \\ Z_1^{L-1} & \vdots & \cdots & Z^{L-1} \end{pmatrix} \quad C = \begin{pmatrix} c_1 & 0 & \cdots & 0 \\ 0 & c_2 & \cdots & 0 \\ \vdots & \vdots & \ddots & \vdots \\ 0 & \vdots & \cdots & c \end{pmatrix} \quad T = \begin{pmatrix} 1 & 1 & \cdots & 1 \\ Z_1^1 & Z_2^1 & \cdots & Z^1 \\ \vdots & \vdots & \ddots & \vdots \\ Z_1^{M-1} & \vdots & \cdots & Z^{M-1} \end{pmatrix}^T$$

where K is the model order to be estimated $L \geq k, M \geq K, N = L + M - 1$.

The p known poles are then indexed as the first one $z, K = 1 \dots, p$ and the rest $z, k = p + 1 \dots, K$ are the unknown poles. Therefore the first p columns S_p and T_p of the of the matrixes S and T are know priory. After QR decomposition of the T_p the data are projected onto the orthogonal subspace.

$$T_p = [Q_1 Q_2] [R^T 0]^T \quad (\text{B.5.1})$$

$$\hat{X} = X Q_2^* = S_{K-p} C_{K-p} T_{K-p}^T Q_2^* \quad (\text{B.5.2})$$

where \hat{X} are the newly projected data, and Q_2^* is the conjugation of Q_2 .

B.6 Parameter estimation algorithm

Step1: Arrange the data points $x_n, n = 1 \dots N - 1$ in a $(L \times M)$ -Hankel matrix \mathbf{H} , $N + L + M - 1, L > K$

$$H = \begin{pmatrix} x_0 & x_1 & \cdots & x_m \\ x_1 & x_2 & \cdots & \\ \vdots & \vdots & \ddots & \vdots \\ x_{L-1} & \vdots & \cdots & x_{N-1} \end{pmatrix} \quad (\text{B.6.1})$$

Step2: Compute the SVD of \mathbf{H}

$$H = U_{Lx\min(L,M)} \sum_{\min(L,M) * \min(L,M)} V_{Mx\min(L,M)}^H \quad (\text{B.6.2})$$

Step3: Truncate the SVD of \mathbf{H} on order to outcome the best rank- K' approximation

$$\hat{H} = \hat{U}_{LxK'} \sum_{K'*K'} \hat{V} V_{MxK'}^H \quad (\text{B.6.3})$$

The rank K' is equal to the model order which correspond to the number of complex exponential in the signal. If the signal is real, then K' is twice the model order.

Step4: Form the overdetermined set of equation

$$\hat{U} \downarrow \approx \hat{U} \uparrow \tilde{Z} \quad (\text{B.6.4})$$

where $\hat{U} \downarrow$ and $\hat{U} \uparrow$ are derived from \hat{U} by omitting its first and last row respectively:

- HSVD: compute an estimate of $\hat{\mathbf{c}}$ by solving the above set of equations via LS
- HTLS: compute an estimate of $\hat{\mathbf{c}}$ by solving the above set of equations via TLS

The eigenvalues λ of \tilde{Z} estimated the poles of the signal $\lambda = \hat{z} = \exp\{-\hat{\alpha} + 2\pi j \hat{v} \delta t\}$ from where it is then very easy the estimation of the damping factor α and the frequencies v .

Step5: Using the estimates $\hat{z}_k, k = 1 \dots, K$ and the signal sample $x_n, n = 0 \dots, N - 1$ compute the LS solution $\hat{\mathbf{c}}_k = \hat{\alpha} \exp\{j\hat{\phi}_k \Delta t\}$

$$\begin{pmatrix} 1 & \cdots & 1 \\ \hat{z}_1^1 & \cdots & \hat{z}_K^1 \\ \vdots & \ddots & \vdots \\ \hat{z}_1^{N-1} & \cdots & \hat{z}_K^{N-1} \end{pmatrix} = \begin{pmatrix} c_1 \\ c_1 \\ \vdots \\ c_K \end{pmatrix} = \begin{pmatrix} x_0 \\ x_1 \\ \vdots \\ x_{N-1} \end{pmatrix} \quad (\text{B.6.5})$$

B.7 Parameter estimation

Table 8: Frequency estimation **Hz**

<i>K</i>	<i>Signal</i>	<i>Cadzow</i>	<i>MV</i>	<i>MCC</i>	<i>OMCC</i>
1	$-9.555977e - 01$	$-9.508942e - 01$	$-9.524330e - 01$	$-9.556628e - 01$	$-9.784238e - 01$
2	$-5.210213e - 01$	$-5.225112e - 01$	$-5.224106e - 01$	$-5.224958e - 01$	$-4.813153e - 01$
3	$-4.775127e - 01$	$-4.772782e - 01$	$-4.771398e - 01$	$-4.810905e - 01$	$-4.336076e - 01$
4	$-4.422597e - 01$	$-4.429406e - 01$	$-4.428970e - 01$	$-4.429050e - 01$	$-4.289482e - 01$
5	$-4.372896e - 01$	$-4.372228e - 01$	$-4.371036e - 01$	$-4.373359e - 01$	$-4.233843e - 01$
6	$-4.228081e - 01$	$-4.227127e - 01$	$-4.227367e - 01$	$-4.230949e - 01$	$-3.385410e - 01$
7	$-3.381981e - 01$	$-3.381209e - 01$	$-3.382215e - 01$	$-3.382721e - 01$	$-3.160027e - 01$
8	$-2.972867e - 01$	$-3.079740e - 01$	$-3.100710e - 01$	$-2.992795e - 01$	$-2.982768e - 01$
9	$-2.084945e - 01$	$-2.085343e - 01$	$-2.085272e - 01$	$-2.570244e - 01$	$-2.085313e - 01$
10	$-1.864170e - 01$	$-1.865248e - 01$	$-1.865114e - 01$	$-2.083074e - 01$	$-1.865894e - 01$
11	$-1.714343e - 01$	$-1.725529e - 01$	$-1.724087e - 01$	$-1.862171e - 01$	$-1.696504e - 01$
12	$-1.626073e - 01$	$-1.622841e - 01$	$-1.622654e - 01$	$-1.735271e - 01$	$-1.622577e - 01$
13	$-1.425370e - 01$	$-1.425430e - 01$	$-1.425451e - 01$	$-1.684904e - 01$	$-1.427893e - 01$
14	$-1.132780e - 01$	$-1.136491e - 01$	$-1.134701e - 01$	$-1.622525e - 01$	$-1.143841e - 01$
15	$-9.452028e - 02$	$-9.513938e - 02$	$-9.510554e - 02$	$-1.425876e - 01$	$-9.433056e - 02$
16	$-6.980151e - 02$	$-6.293848e - 02$	$-6.332083e - 02$	$-1.148028e - 01$	$-6.850752e - 02$
17	$-4.262248e - 02$	$-3.891636e - 02$	$-3.960942e - 02$	$-9.779944e - 02$	$-4.176006e - 02$
18	$-2.996232e - 02$	$-2.969594e - 02$	$-2.972182e - 02$	$-9.584091e - 02$	$-1.730952e - 03$
19	$4.473684e - 03$	$4.665877e - 03$	$4.698955e - 03$	$-3.957121e - 02$	$4.542893e - 03$
20	$6.077749e - 03$	$6.324578e - 03$	$6.300752e - 03$	$-3.260423e - 03$	$6.193991e - 03$
21	$1.048974e - 02$	$1.075331e - 02$	$1.074913e - 02$	$5.049077e - 03$	$1.071062e - 02$
22	$2.215293e - 02$	$2.219276e - 02$	$2.218440e - 02$	$6.612468e - 03$	$1.449617e - 02$
23	$4.611676e - 02$	$4.631646e - 02$	$4.632130e - 02$	$1.073775e - 02$	$2.199675e - 02$
24	$2.447092e - 01$	$2.446299e - 01$	$2.446276e - 01$	$2.209951e - 02$	$2.790690e - 02$
25	$4.509877e - 01$	$4.509306e - 01$	$4.509305e - 01$	$4.596468e - 02$	$3.769979e - 02$
26	$5.621533e - 01$	$5.638890e - 01$	$5.638999e - 01$	$4.507900e - 01$	$4.664923e - 02$
27	$7.165705e - 01$	$7.170652e - 01$	$7.170643e - 01$	$7.160317e - 01$	0
28	$8.687320e - 01$	$9.173103e - 01$	$9.173219e - 01$	$9.174260e - 01$	0

Table 9: Damping estimation **Hz**

<i>K</i>	<i>Signal</i>	<i>Cadzow</i>	<i>MV</i>	<i>MCC</i>	<i>OMCC</i>
1	$3.805591e + 00$	$3.864923e + 00$	$3.878156e + 00$	$3.789683e + 00$	$4.123024e + 00$
2	$1.818921e - 03$	$1.408335e - 03$	$1.437382e - 03$	$1.495179e - 03$	$7.444401e - 02$
3	$4.042687e - 02$	$4.704333e - 02$	$4.772579e - 02$	$5.386269e - 02$	$9.976213e - 02$
4	$-1.048773e - 04$	$-7.288015e - 04$	$-6.853811e - 04$	$-6.064308e - 04$	$4.043913e - 02$
5	$5.294169e - 02$	$5.109968e - 02$	$5.112902e - 02$	$4.669877e - 02$	$1.338776e - 02$
6	$7.528497e - 05$	$9.063004e - 04$	$8.517528e - 04$	$1.134128e - 03$	$2.288375e - 02$
7	$2.565433e - 02$	$2.076901e - 02$	$1.993093e - 02$	$2.423329e - 02$	$6.003181e - 02$
8	$9.728549e - 02$	$1.636937e - 01$	$1.802259e - 01$	$1.030646e - 01$	$6.578056e - 02$
9	$1.644666e - 02$	$1.660806e - 02$	$1.655827e - 02$	$1.164466e - 02$	$1.624612e - 02$
10	$2.145536e - 02$	$2.176431e - 02$	$2.178176e - 02$	$1.629567e - 02$	$2.206827e - 02$
11	$1.743023e - 03$	$2.294497e - 03$	$2.645388e - 03$	$2.092555e - 02$	$1.766815e - 02$
12	$8.520057e - 04$	$8.237712e - 04$	$9.081262e - 04$	$2.121525e - 03$	$2.770686e - 03$
13	$1.206222e - 02$	$1.255893e - 02$	$1.266137e - 02$	$7.271317e - 03$	$1.183997e - 02$
14	$3.792665e - 02$	$4.419109e - 02$	$4.598252e - 02$	$1.296224e - 03$	$3.434041e - 02$
15	$3.484462e - 02$	$3.320853e - 02$	$3.350006e - 02$	$1.064895e - 02$	$2.903771e - 02$
16	$1.675940e - 02$	$4.933585e - 03$	$6.503359e - 03$	$1.830517e - 02$	$4.682061e - 02$
17	$7.981585e - 03$	$1.206486e - 02$	$1.311986e - 02$	$1.011961e - 01$	$9.504811e - 03$
18	$1.128859e - 03$	$9.386782e - 04$	$1.049957e - 03$	$1.527209e - 02$	$-1.959978e - 03$
19	$-1.097017e - 03$	$-1.439230e - 03$	$-1.432994e - 03$	$7.949442e - 03$	$-1.842160e - 03$
20	$-5.156887e - 04$	$-5.597176e - 04$	$-5.725033e - 04$	$-4.304302e - 03$	$-1.032574e - 03$
21	$-1.210555e - 03$	$-1.892206e - 03$	$-1.904945e - 03$	$-1.234197e - 03$	$-1.270581e - 03$
22	$2.576451e - 03$	$1.341022e - 03$	$1.416227e - 03$	$-5.355918e - 04$	$2.705122e - 03$
23	$2.001404e - 03$	$4.611936e - 03$	$4.646519e - 03$	$-2.309088e - 03$	$3.296107e - 03$
24	$-4.320644e - 04$	$-8.272031e - 04$	$-8.253756e - 04$	$1.209954e - 03$	$-2.615617e - 04$
25	$-1.065008e - 03$	$-1.233190e - 03$	$-1.239737e - 03$	$4.864949e - 03$	$1.588047e - 02$
26	$2.294689e - 03$	$1.201276e - 03$	$1.225605e - 03$	$-1.300730e - 03$	$8.342141e - 03$
27	$-1.653320e - 03$	$-3.188832e - 03$	$-3.186573e - 03$	$-2.635587e - 03$	$0 \quad 0$
28	$6.284441e - 03$	$2.717628e - 03$	$2.988082e - 03$	$2.506672e - 03$	$0 \quad 0$

Table 10: Amplitude estimation **a.u**

<i>K</i>	<i>Signal</i>	<i>Cadzow</i>	<i>MV</i>	<i>MCC</i>	<i>OMCC</i>
1	$3.256640e + 01$	$3.300156e + 01$	$3.241067e + 01$	$3.273161e + 01$	$3.316891e + 01$
2	$5.422893e - 03$	$1.336719e - 02$	$1.075945e - 02$	$1.365091e - 02$	$7.757696e - 01$
3	$4.099552e - 01$	$4.492171e - 01$	$4.018871e - 01$	$5.221275e - 01$	$2.664435e + 00$
4	$5.014596e - 03$	$5.014298e - 03$	$4.179407e - 03$	$5.118421e - 03$	$1.102910e + 00$
5	$1.150562e + 00$	$1.068390e + 00$	$1.025071e + 00$	$9.808967e - 01$	$1.456264e - 01$
6	$5.292357e - 03$	$9.167744e - 03$	$7.403087e - 03$	$9.990511e - 03$	$7.669006e - 01$
7	$8.488216e - 01$	$6.781531e - 01$	$6.352379e - 01$	$7.986466e - 01$	$3.442866e - 01$
8	$1.006942e + 00$	$1.603732e + 00$	$1.635733e + 00$	$9.966566e - 01$	$6.168837e - 01$
9	$4.852307e - 01$	$4.908373e - 01$	$4.792482e - 01$	$6.912732e - 02$	$4.810633e - 01$
10	$6.244920e - 01$	$6.378518e - 01$	$6.250894e - 01$	$4.841901e - 01$	$6.540142e - 01$
11	$1.267314e - 02$	$1.808945e - 02$	$1.753342e - 02$	$6.212662e - 01$	$8.518966e - 02$
12	$9.966341e - 03$	$1.348542e - 02$	$1.214601e - 02$	$1.640881e - 02$	$2.876379e - 02$
13	$1.788077e - 01$	$1.877151e - 01$	$1.758072e - 01$	$4.082911e - 02$	$1.697590e - 01$
14	$6.013779e - 01$	$7.046168e - 01$	$6.863502e - 01$	$1.766735e - 02$	$4.949241e - 01$
15	$8.679509e - 01$	$8.106876e - 01$	$7.922108e - 01$	$1.598442e - 01$	$6.764973e - 01$
16	$1.021373e - 01$	$3.658203e - 02$	$3.652253e - 02$	$2.123959e - 01$	$2.533458e - 01$
17	$4.772593e - 02$	$8.532346e - 02$	$7.400564e - 02$	$1.447198e + 00$	$4.069183e - 02$
18	$1.050509e - 02$	$1.054224e - 02$	$9.148235e - 03$	$2.628179e - 01$	$6.270791e - 04$
19	$4.974141e - 03$	$4.354608e - 03$	$3.818156e - 03$	$4.246921e - 02$	$2.472780e - 03$
20	$7.095809e - 03$	$7.733197e - 03$	$6.811282e - 03$	$3.431183e - 04$	$4.454147e - 03$
21	$4.137996e - 03$	$3.021816e - 03$	$2.489087e - 03$	$4.762895e - 03$	$9.890000e - 04$
22	$2.508088e - 02$	$1.769941e - 02$	$1.505020e - 02$	$5.583697e - 03$	$1.597420e - 02$
23	$2.874834e - 02$	$4.715150e - 02$	$4.200023e - 02$	$1.778808e - 03$	$1.840909e - 02$
24	$5.007011e - 03$	$5.342626e - 03$	$4.356132e - 03$	$1.596865e - 02$	$3.190921e - 03$
25	$3.448467e - 03$	$3.733743e - 03$	$2.930326e - 03$	$4.995066e - 02$	$6.893042e - 02$
26	$5.341363e - 03$	$1.366129e - 02$	$1.076499e - 02$	$3.474173e - 03$	$6.816109e - 02$
27	$1.024626e - 03$	$5.608500e - 04$	$4.454651e - 04$	$7.562295e - 04$	$0 \quad 0$
28	$1.200869e - 02$	$1.954046e - 02$	$1.624438e - 02$	$2.079175e - 02$	$0 \quad 0$

Table 11: Phase estimation **Deg**

<i>K</i>	<i>Signal</i>	<i>Cadzow</i>	<i>MV</i>	<i>MCC</i>	<i>OMCC</i>
1	$1.855057e + 02$	$1.854082e + 02$	$1.854481e + 02$	$1.850640e + 02$	$1.871292e + 02$
2	$9.810874e + 01$	$1.876224e + 02$	$1.763864e + 02$	$1.866469e + 02$	$3.328751e + 02$
3	$3.246461e + 02$	$3.197151e + 02$	$3.191388e + 02$	$3.395757e + 02$	$4.108068e + 01$
4	$2.701932e + 02$	$4.780873e + 01$	$3.705940e + 01$	$3.740396e + 01$	$2.311594e + 02$
5	$1.135763e + 01$	$8.187054e + 00$	$7.303432e + 00$	$1.081422e + 01$	$3.226268e + 02$
6	$2.924741e + 02$	$2.765652e + 02$	$2.793982e + 02$	$3.125822e + 02$	$3.505516e + 02$
7	$3.471741e + 02$	$3.418714e + 02$	$3.434347e + 02$	$3.465695e + 02$	$3.127268e + 02$
8	$3.248599e + 02$	$3.363620e + 02$	$3.367679e + 02$	$3.234797e + 02$	$3.526643e + 02$
9	$3.282290e + 02$	$3.303960e + 02$	$3.302554e + 02$	$2.637392e + 02$	$3.304806e + 02$
10	$3.516400e + 02$	$3.545322e + 02$	$3.542989e + 02$	$3.247032e + 02$	$3.562212e + 02$
11	$1.051530e + 02$	$1.578982e + 02$	$1.516360e + 02$	$3.480910e + 02$	$8.963210e + 01$
12	$1.776165e + 02$	$1.375745e + 02$	$1.342497e + 02$	$2.482518e + 02$	$1.416245e + 02$
13	$3.449026e + 02$	$3.432946e + 02$	$3.435226e + 02$	$4.611104e + 01$	$3.515427e + 02$
14	$3.248060e + 02$	$3.322843e + 02$	$3.309917e + 02$	$1.340965e + 02$	$3.399520e + 02$
15	$3.449528e + 02$	$3.533976e + 02$	$3.529525e + 02$	$3.438892e + 02$	$3.399204e + 02$
16	$3.026402e + 02$	$2.759712e + 02$	$2.796225e + 02$	$3.313282e + 02$	$2.854151e + 02$
17	$2.832686e + 02$	$2.330660e + 02$	$2.402000e + 02$	$3.253930e + 02$	$2.835442e + 02$
18	$1.485587e + 02$	$9.957196e + 01$	$1.033912e + 02$	$2.124476e + 01$	$1.880107e + 02$
19	$2.471890e + 02$	$2.031435e + 02$	$1.955784e + 02$	$2.459106e + 02$	$2.368190e + 02$
20	$2.676863e + 02$	$2.200820e + 02$	$2.248424e + 02$	$3.419659e + 02$	$2.425510e + 02$
21	$6.164143e + 01$	$3.552336e + 02$	$3.561116e + 02$	$1.179184e + 02$	$3.404062e + 02$
22	$1.992717e + 02$	$2.040184e + 02$	$2.043274e + 02$	$1.668620e + 02$	$2.845547e + 02$
23	$2.375201e + 02$	$2.226361e + 02$	$2.221898e + 02$	$4.854302e + 00$	$2.114117e + 02$
24	$2.641042e + 02$	$2.856466e + 02$	$2.863055e + 02$	$2.174271e + 02$	$2.646670e + 02$
25	$4.720148e + 01$	$6.655024e + 01$	$6.648823e + 01$	$2.409339e + 02$	$6.690049e + 01$
26	$3.564086e + 02$	$3.346186e + 02$	$3.324396e + 02$	$9.985507e + 01$	$2.080372e + 02$
27	$7.789302e + 01$	$3.157860e + 02$	$3.160813e + 02$	$3.225183e + 02$	0 0
28	$1.081902e + 02$	$2.238771e + 01$	$2.219750e + 01$	$1.009060e + 01$	0 0

B.8 Signal enhancement algorithm

Step1: Arrange the data points $x_n, n = 1 \dots N - 1$ in a $(L \times M)$ -Hankel matrix \mathbf{H} , $N + L + M - 1, L > K$

$$H = \begin{pmatrix} x_0 & x_1 & \cdots & x_m \\ x_1 & x_2 & \cdots & \\ \vdots & \vdots & \ddots & \vdots \\ x_{L-1} & \vdots & \cdots & x_{N-1} \end{pmatrix} \quad (\text{B.8.1})$$

Step2: Compute the SVD of \mathbf{H}

$$H = U_{Lx\min(L,M)} \Sigma_{\min(L,M)*\min(L,M)} V_{Mx\min(L,M)}^H \quad (\text{B.8.2})$$

Step3: Truncate the SVD of \mathbf{H} on order to outcome the best rank- K' approximation

$$\hat{H} = \hat{U}_{LxK'} f\{\hat{\Sigma}_{K'*K'}\} \hat{V}_{MxK'}^H \quad (\text{B.8.3})$$

The rank K' is equal to the model order which correspond to the number of complex exponential in the signal. If the signal is real, then K' is twice the model order. The correction is different of the singular values is $f\{\hat{\Sigma}_{K'*K'}\} = (\Sigma_1)$ for Cadzow and $f\{\hat{\Sigma}_{K'*K'}\} = (\Sigma_1^2 - L\sigma_w^2 I_K) \Sigma_1^{-1}$ for MV.

Step4: Average along the anti-diagonal the the reconstructed matrix which leads to a the Hankel matrix

$$\hat{H}_{\text{ant-diag-ave}} = \text{Average}(\hat{H}) \quad (\text{B.8.4})$$

Step5: Extract the first column and the last row of the newly computed Hankel matrix $\hat{H}_{\text{ant-diag-ave}}$

B.9 Multi channel signal enhancement algorithm

Step1: Arrange the data points $x_n^q, n = 1 \dots N - 1$ in a $(L \times M)$ -Hankel matrix \mathbf{H} , $N + L + M - 1, L > K$ for all the channel data $q = 1 \dots Q$

$$H_1 = \begin{pmatrix} x_0 & x_1 & \cdots & x_m \\ x_1 & x_2 & \cdots & \\ \vdots & \vdots & \ddots & \vdots \\ x_{L-1} & \vdots & \cdots & x_{N-1} \end{pmatrix} \dots \dots H_Q = \begin{pmatrix} x_0 & x_1 & \cdots & x_m \\ x_1 & x_2 & \cdots & \\ \vdots & \vdots & \ddots & \vdots \\ x_{L-1} & \vdots & \cdots & x_{N-1} \end{pmatrix} \quad (\text{B.9.1})$$

Step2: Form a block Hankel matrix

$$H = [H_1 | H_2 | \dots | H_Q] \quad (\text{B.9.2})$$

Step3: Compute the SVD of \mathbf{H}

$$H = U_{Lx\min(L,M)} \Sigma_{\min(L,M)*\min(L,M)} V_{Mx\min(L,M)}^H \quad (\text{B.9.3})$$

Step4: Truncate the SVD of \mathbf{H} on order to outcome the best rank- K' approximation

$$\hat{H} = \hat{U}_{LxK'} f\{\hat{\Sigma}_{K'*K'}\} \hat{V}_{MxK'}^H \quad (\text{B.9.4})$$

The rank K' is equal to the model order which correspond to the number of complex exponential in the signal. If the signal is real, then K' is twice the model order. The correction is different of the singular values is $f\{\hat{\Sigma}_{K'*K'}\} = (\Sigma_1)$ for Cadzow and $f\{\hat{\Sigma}_{K'*K'}\} = (\Sigma_1^2 - L\sigma_w^2 I_K) \Sigma_1^{-1}$ for MV.

Step5: Average along the anti-diagonal the the reconstructed matrix \hat{H} which leads to a the the Hankel matrix

$$\hat{H}_{ant-diag-ave} = \text{Average}(\hat{H}) \quad (\text{B.9.5})$$

Step5: Extract the the Hankel matrix corresponding to the voxel of interest $H_{interest}$

Step6: Extract the first column and the last row of the newly computed Hankel matrix $H_{interest}$

B.10 Parameter estimation

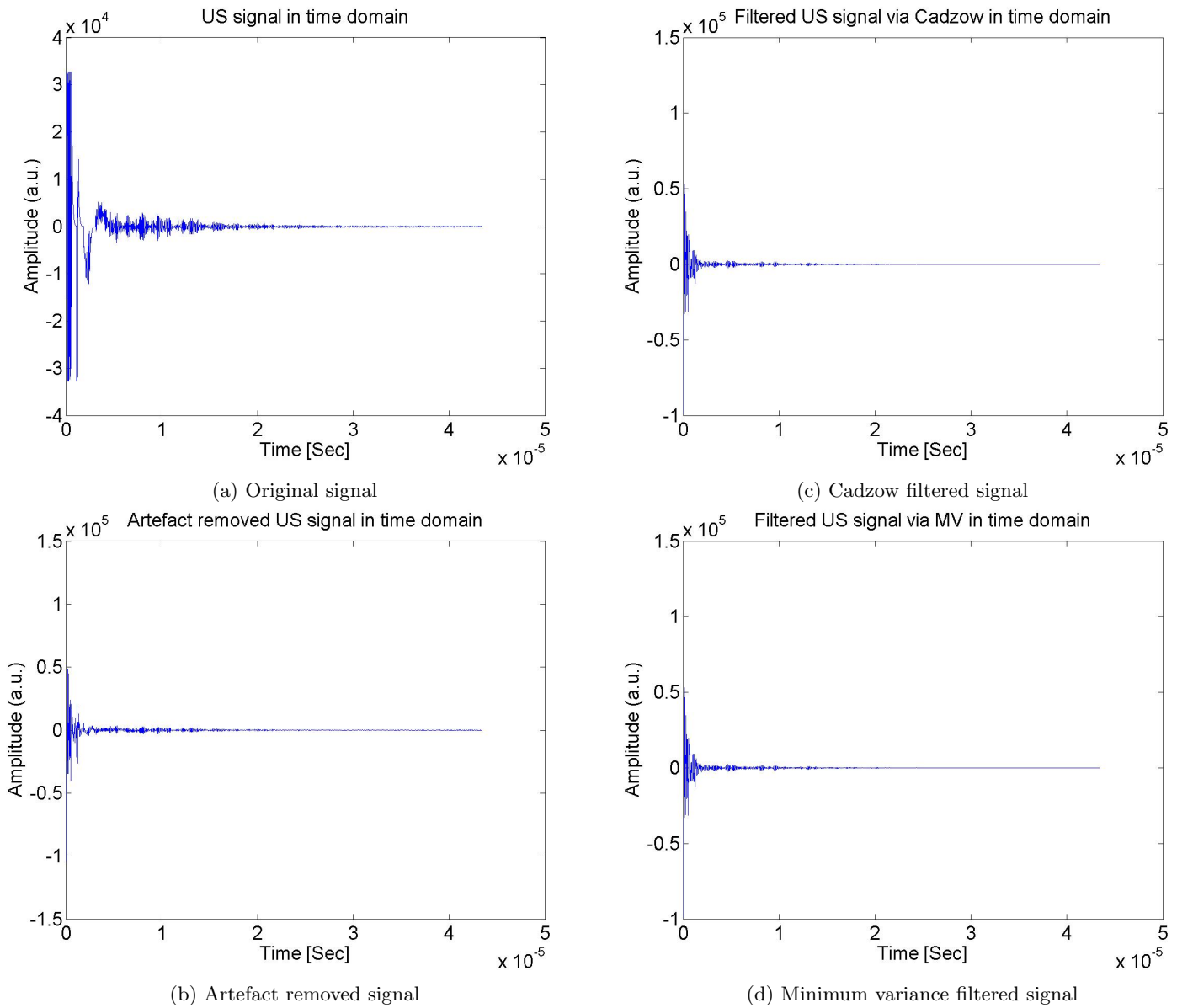


Figure B.10.1: Time domain signal

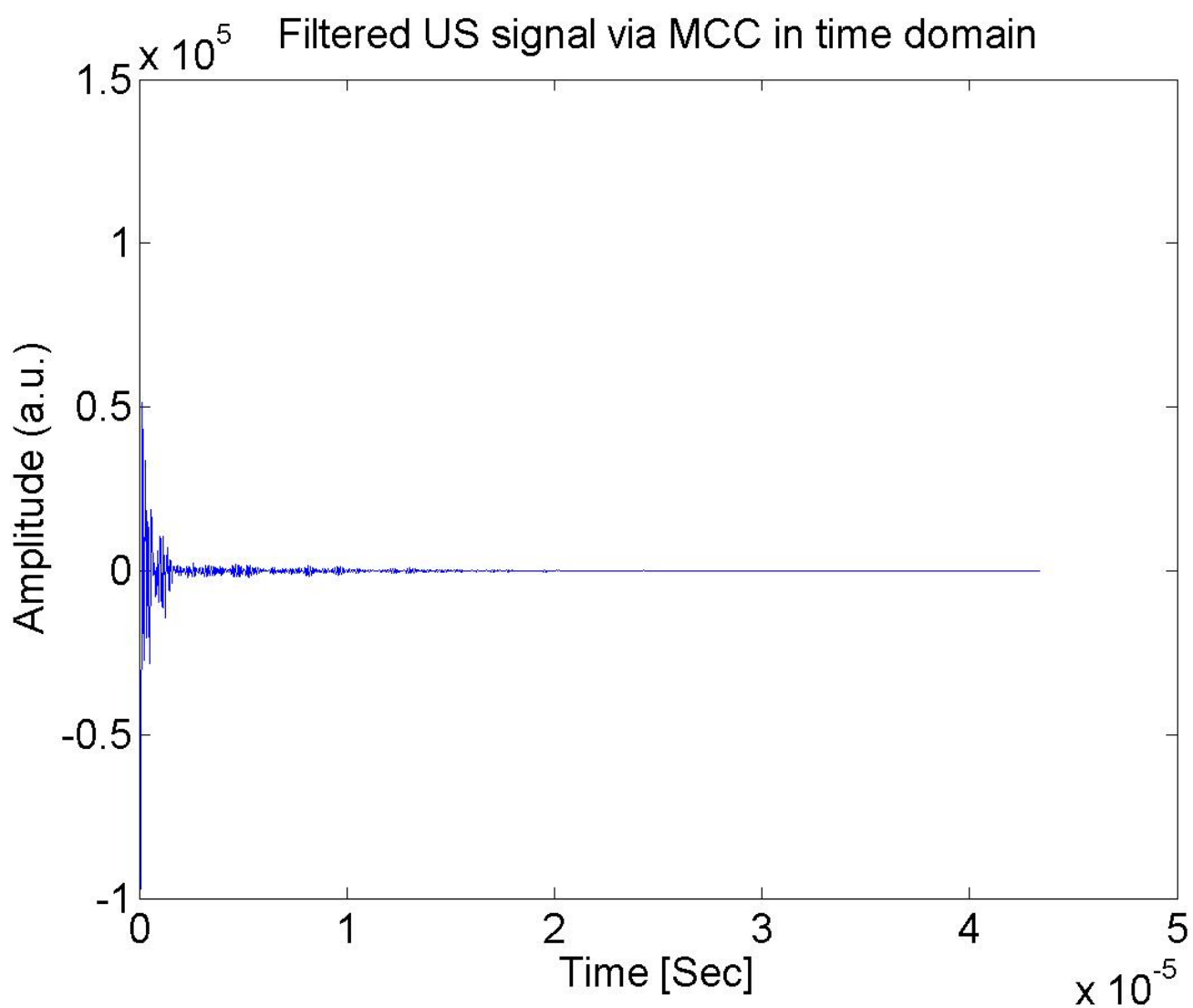


Figure B.10.2: Multichnnale outcome